The control exerted by ABA on lignan biosynthesis in flax (Linum usitatissimum L.) is modulated by a Ca2+ signal transduction involving the calmodulin-like LuCML15b

Lucija Markulin, Samantha Drouet, Cyrielle Corbin, Cédric Decourtil, Laurine Garros, Sullivan Renouard, Tatiana Lopez, Gaëlle Mongélard, Laurent Gutierrez, Daniel Auguin, et al.

The control exerted by ABA on lignan biosynthesis in flax (*Linum usitatissimum* L.) is modulated by a Ca^{2+} signal transduction involving the calmodulin-like LuCML15b

Lucija Markulin[12§], Samantha Drouet[12§], Cyrielle Corbin[12§], Cédric Decourtil[12], Laurine Garros[12], Sullivan Renouard[12], Tatiana Lopez[12], Gaëlle Mongelard[3], Laurent Gutierrez[3], Daniel Auguin[12], Eric Lainé[12†], Christophe Hano[12†*]

[1] Laboratoire de Biologie des Ligneux et des Grandes Cultures (LBLGC), INRA, USC1328, Université d'Orléans, Pôle Universitaire d'Eure et Loir, 21 rue de Loigny la Bataille, F-28000 Chartres, France

[2] Bioactifs et Cosmétiques, GDR 3711 COSMACTIFS, CNRS Université d'Orléans, rue de Chartres, F-45100 Orléans, France

[3] Centre de Ressources Régionales en Biologie Moléculaire (CRRBM), Université Picardie Jules Verne, 33 rue Saint-Leu, F-80039 Amiens, France

[§] These authors contributed equally to this work and should be considered both as first authors

[†] These authors have equal contribution of the senior authors.

[*] To whom correspondence should be addressed: Dr Christophe Hano
LBLGC EA1207, INRA USC1328, CNRS GDR3711, Plant LIGNANS Team, Université d'Orléans, Pôle Universitaire d'Eure et Loir, 21 rue de Loigny la Bataille, 28000 Chartres, France ; Tel.: + 33 2 37 30 97 53; Fax: +33 2 37 91 08 63; E-mail: hano@univ-orleans.fr

Abstract

The *LuPLR1* gene encodes a pinoresinol lariciresinol reductase responsible for the biosynthesis of (+)-secoisolariciresinol, a cancer chemopreventive lignan, highly accumulated in the seedcoat of flax (*Linum usitatissimum* L.). Abscisic acid (ABA) plays a key role in the regulation of *LuPLR1* gene expression and lignan accumulation in both seeds and cell suspensions, which require two *cis*-acting elements (ABRE and MYB2) for this regulation. Ca^{2+} is a universal secondary messenger involved in a wide range of physiological processes including ABA signaling. Therefore, Ca^{2+} may be involved as a mediator of *LuPLR1* gene expression and lignan biosynthesis regulation exerted by ABA. To test the potential implication of Ca^{2+} signaling, a pharmacological approach was conducted using both flax cell suspensions and maturing seed systems coupled with a ß-glucuronidase reporter gene experiment, RT-qPCR analysis, lignan quantification as well as Ca^{2+} fluorescence imaging. Exogenous ABA application results in an increase in the intracellular Ca^{2+} cytosolic concentration, originating mainly from the extracellular medium. Promoter-reporter deletion experiments suggest that the ABRE and MYB2 *cis*-acting elements of the *LuPLR1* gene promoter functioned as Ca^{2+}-sensitive sequences involved in the ABA-mediated regulation. The use of specific inhibitors pointed the crucial roles of the Ca^{2+} sensors calmodulin-like proteins and Ca^{2+}-dependent protein kinases in this regulation. This regulation appeared conserved in the two different studied systems, i.e. cell suspensions and maturing seeds. A calmodulin-like, LuCML15b, identified from gene network analysis is proposed as a key player involved in this signal transduction since RNAi experiments provided direct evidences of this role. Taken together, these results provide new information on the regulation of plant defense and human health-promoting compounds, which could be used to optimize their production.

Keywords: Abscisic acid, Calcium, Calmodulin, Flax, Lignan, Pinoresinol-lariciresinol reductase

1. Introduction

Over the last decades, flax seed coat lignans have been of growing significance, particularly for their numerous benefits on human health (Lainé et al., 2009; Oomah, 2001; Westcott and Muir, 2003). Lignans are an important class of 8-8′ linked phenylpropanoid (C_6C_3) dimers widely distributed across the vascular plants. They are supposed to play a role in plant defense (Corbin et al., 2017; Gang et al., 1999). Flaxseeds represent one of the richest source and are considered as an attractive model to study lignan biochemical and/or physiological functions, particularly since its seed coats accumulate (+)-secoisolariciresinol lignan derivatives in high amount. However, flaxseed lignans have been well studied and characterized for their beneficial properties on human health (Hano et al., 2013; Lainé et al., 2009) but their physiological functions and regulation of biosynthesis *in planta* remain elusive. The direct *in vivo* implication of the *LuPLR1* gene and its rate-limiting action on (+)-secoisolariciresinol diglucoside (SDG) biosynthesis has been evidenced by RNAi technology applied to the down-regulation of the *LuPLR1* gene expression in developing flax seeds (Renouard et al., 2014). Its gene expression regulation by abscisic acid (ABA) during seed maturation and in flax cell suspensions have been evidenced (Corbin et al., 2013b, 2013a; Renouard et al., 2012a). On the contrary, a second PLR isoform (i.e., LuPLR2) was functionally characterized in flax, and its involvement in the biosynthesis of (-)-yatein, a lignan deriving from the opposite (-)-secoisolariciresinol enantiomer, in flax leaves evidenced (Corbin et al., 2017). However, the end product of this alternative pathway (-)-yatein is barely detectable in both flax seeds and cell suspensions, whereas (-)-secoisolariciresinol, the LuPLR2 product, is only accumulated in minor amount in seed and not detected in cell suspension (Corbin et al., 2017; Corbin et al., 2018).

In plants, ABA plays a critical role in the regulation of seed development and maturation but is also involved in other physiological and developmental processes such as seedling growth, flowering or environmental adaptation to biotic stress or abiotic stress such as drought, salt and cold (Finkelstein et al., 2002; Frey et al., 2004; Gutierrez et al., 2007). As many as 10% of the genes of *Arabidopsis thaliana* are responsive to ABA (Finkelstein et al., 2002), some of which are associated with seed development, maturation processes or stress responses such as those involved in the phenylpropanoid pathway (Finkelstein et al., 2002).

ABA actions are mediated by changes in the expression of target genes harboring specific *cis*-acting elements in their promoters (Abe et al., 2003; Busk and Pagès, 1998; Finkelstein et al., 2002; Gutierrez et al., 2007). Such *cis*-acting elements have been identified and characterized

84 in the promoter of the *LuPLR1* gene encoding the pinoresinol lariciresinol reductase involved
85 in the biosynthesis of (+)-secoisolariciresinol, the main lignan under its diglucoside form
86 accumulated in flax seeds (Hano et al., 2006b). Studies with immature flaxseed or cell
87 cultures, have evidenced an ABA-mediated transcriptional activation of the *LuPLR1* gene
88 acting through two important *cis*-acting sequences (ABRE and MYB2) (Corbin et al., 2013a,
89 2013b, Renouard et al., 2014, 2012b).
90 Calcium (Ca^{2+}) is known to be an important second messenger in abscisic acid (ABA) signal
91 transduction, through the action of Ca^{2+} sensors including Ca^{2+}-dependent protein kinases
92 (CDPKs), calmodulin (CaM) and CaM-related proteins (Zhao et al., 2011b). Ca^{2+} is a
93 ubiquitous secondary messenger involved in a wide range of signaling cascades (Lecourieux
94 et al., 2006) and a convergence point of many different signaling pathways (Tuteja and
95 Mahajan, 2007) especially in development and stress (Arimura and Maffei, 2010; Hepler,
96 2005; Reddy et al., 2011). This ion could represent up to 5% of the plant dry weight (White
97 and Broadley, 2003) but could be very toxic at high concentrations so its cytoplasmic
98 concentration should be tightly controlled at both temporal and spatial levels. Consequently,
99 there is a gradient of concentration on both sides of the plasma membrane with a high Ca^{2+}
100 concentration in the extracellular medium, as well as in cellular organelles such as the central
101 vacuole, which represents the largest intracellular Ca^{2+} store (Batistič and Kudla, 2012;
102 Pottosin and Schönknecht, 2007). Upon signal perception, a transient increase occurs in the
103 intracellular Ca^{2+} concentration, triggering a signaling cascade (Batistič and Kudla, 2012;
104 Tuteja, 2009). These cytosolic Ca^{2+} ions could originate from either extracellular or
105 intracellular stores and the use of specific Ca^{2+} channel inhibitors or extracellular chelators
106 enables their origin to be determined.
107 To date there is only few examples for the role of Ca^{2+} signaling in the regulation of plant
108 secondary metabolism and no one reports on lignan (*sensu stricto*) biosynthesis. The
109 transcriptional regulation of the genes related to lignan biosynthesis has been investigated
110 rarely although such data could yield information about the role of these compounds *in*
111 *planta.* Here, we explored the possible involvement of Ca^{2+} ion fluxes and Ca^{2+} signaling in
112 this ABA-mediated transcriptional regulation of the lignan biosynthesis in flax cell
113 suspensions and maturing seeds.
114

2. Materials and Methods

2.1. Plant materials

All flax (*Linum usitatissimum* L.) plant material was generated from the linseed cultivar Barbara supplied by Coopérative Terre de Lin (St Pierre le Viger, France). The wild type LuCY1 and the transgenic promoter *LuPLR1*:GUS (*uidA* ß-glucuronidase reporter gene under the control of the complete version of the *LuPLR1* gene promoter) are cell suspension cultures of *Linum usitatissimum* cv Barbara established from hypocotyl-derived calli and cultured in M2 medium derived from the MS medium (Murashige and Skoog, 1962) supplemented with 3% (w/v) sucrose, 8.88 µM benzylaminopurine and 2.68 µM α-naphthalene acetic acid but depleted or modified in Ca^{2+} concentration for the requirements of the experiments. All suspension cultures were incubated on a gyratory shaker at 120 rpm in darkness at 25°C and subcultured every 14 days as described in Hano et al. (2006a) (Hano et al., 2006a) with 5 g of cells in 100 ml of medium in 250 ml Erlenmeyer flasks.

2.2. Plasmid constructs

Mutated versions of the *LuPLR1* gene promoter in which the ABRE and/or MYB2 *cis*-acting elements were disrupted (described in (Corbin et al., 2013b)).

RNAi vector targeting CML15b (Lus10027243) was obtained as follow: a 155bp fragment of the CML15b coding was amplified by PCR using the following specific primers: iCML15b-F (5'-CACCGTTCGATAGGGACGGGAAC-3' and iCML15b-R (5'-TCGAGAACTCCGTGAAGCTAA-3'), purified (Gel extraction kit, Thermo) and subcloned into the pENTR/D TOPO cloning vector (Invitrogen) following the manufacturer's recommendations. This target sequence was designed using the pssRNAit server tool dedicated to the design of effective and specific (limiting off-target silencing) and non-toxic siRNAs for plant RNAi (Dai and Zhao, 2011). The resulting constructs was then used for transfer into the pP7FWG2 destination vector (Karimi et al., 2002) by using the Gateway technology (Invitrogen) to obtain the iCML15b vector (T-DNA scheme). The construct was sequenced (MWG Biotech). The plasmids were then transferred into the disarmed *A. tumefaciens* strain GV3101 (pGV2260) with *E. coli* strain HB101 (pRK2013) as helper.

2.3. Transient cell transformation

The protocol for transient expression described by Berger et al. (2007) (Berger et al., 2007) were used. Briefly, a single colony of *A. tumefaciens* strain GV3101 with the binary vector

was inoculated into YEB liquid medium containing 50 mg ml^{-1} kanamycin and grown at 28°C in a gyratory shaker (180 rpm) to an absorbance of 1.5 at 600 nm. Bacterial cells were harvested by centrifugation at 6,000 *g* for 5 min and washed twice with 10 ml of fresh M2 culture medium. After 5 min of centrifugation at 6,000 *g*, the pellet of bacterial cells was resuspended in 1 ml of medium containing 20 µM acetosyringone (Sigma, St Quentin Fallavier, France). Ten-day-old flax cell suspensions were harvested by centrifugation at 3,000 *g* for 5 min, rinsed three times with buffer medium and resuspended at a 1:4 dilution in 2.5 ml of fresh buffer medium in six-well sterile culture plates. Fifty µl of the resuspended bacterial cells was added to the flax cell suspension. After 24 h of co-culture (dark, 25°C, 120 rpm), each cell suspension was treated with chemicals.

2.4. Chemicals and cell suspension treatments

All chemicals used in the present study were purchased from Sigma (St Quentin Fallavier, France). After the exponential growth phase (day 10), cell suspension cultures were transferred into the incubation medium (0.5 M mannitol, 10 mM PIPES, pH 5.8) and subjected to the different chemical treatments. The same volume (25 µL) of 100X concentrated stock solution of each chemical reagent (dissolved in DMSO and diluted with incubation buffer at the mentioned concentration) was added to 2.5 ml of cell suspension (125 mg) cultured in sterile six-well culture plates. Control cells were inoculated with the same volume of DMSO-containing-buffer medium. Microplates were maintained on a gyratory shaker at 120 rpm in darkness at 25°C. Cells were observed under a microscope or collected 24 h after treatment for RNA extraction and gene expression measurement, 48 h for β-glucuronidase analysis and 96 h for lignan quantification by centrifugation at 3,000 *g* for 10 min and stored at -80°C until further analysis. The growth of cell suspensions during a cycle was measured by the packed cell volume (PCV) method. Briefly, PCV was determined following centrifugation of 20 mL of cell suspension in a graduated conical centrifuge tube of 50 mL at 200 g for 5 min. The volume of sedimented cells was measured and the PCV was calculated as percentage of sedimented cells vs total volume.

2.5. Immature seed treatments

Capsules containing immature developing flaxseeds (stage 2, (Hano et al., 2006b)) were submitted to exogenous administration of (±) *cis–trans* ABA (50 µM) combined or not with staurosporine (5 µM) or calmidazolium (25 µM) as described by Renouard et al. (2012)

(Renouard et al., 2012b). Briefly, secondary inflorescence stems of wild or transgenic flax plants (stage 2) were harvested and placed directly in deionized water. Capsules with a remaining peduncle (around 1 cm) were pruned from stems and immediately size-sorted. Three fresh capsules for each treatment were placed in one well of a 96-well microplate and maintained at 25°C under a 16-h photoperiod. After uptake, capsules were dissected, and seeds (*ca*. 60 per condition) were stored at −80°C until their use for RT-qPCR and phytochemical analysis ((+)-secoisolariciresinol and ABA contents).

2.6. β-glucuronidase activity

β-glucuronidase (GUS) activity assays were performed by measuring 4-methylumbelliferone (4-MU, Sigma, St Quentin Fallavier, France) produced from the glucuronide precursor 4-methylumbelliferyl-β-D-glucuronide (4-MUG, Sigma, St Quentin Fallavier, France). Fifty mg of cells were ground and homogenized in 500 µl of extraction buffer containing 50 mM sodium phosphate; pH 7.0, 10 mM EDTA, 0.1% (v/v) Triton X-100, 0.1% sarcosyl, and 10 mM β-mercaptoethanol at 4°C. Following 15 min of centrifugation at 12,000 *g* at 4°C, GUS activity was quantified in the supernatant using a fluorescence spectrophotometer (BioRad, Marnes-la-Coquette, France). Protein concentrations were determined using a fluorometer and the Quant-iT Protein Assay Kit (Invitrogen) adapted for the Qubit fluorometer according to the manufacturer's protocol. β-glucuronidase activity was expressed as RFU (Relative Fluorescence Unit) per mg of soluble proteins.

2.7. RNA extraction and quantitative PCR

Total RNA was extracted from 100 mg of ground frozen tissues using the RNeasy Plant Kit (Qiagen, Courtabeuf, France) and the RNase free DNase set (Qiagen, Courtabeuf, France) in order to eliminate DNA contamination, as described in Hano et al. (2006b) (Hano et al., 2006b). RNAs were quantified using a fluorometer and the Quant-iT RNA Assay Kit (Invitrogen) adapted for the Qubit fluorometer according to the manufacturer's protocol. Reverse transcription was performed using the First-strand cDNA synthesis kit (Thermo, Villebon sur Yvette, France).

Quantitative PCR was performed in 96-well plates with a PikoReal real time PCR system (ThermoFisher) using the DyNAmoColorFlash SYBR Green qPCR Kit (ThermoFisher, Villebon sur Yvette, France). The reaction was carried out in 20 µL (1 µL diluted cDNAs, 10 µL of 2x SYBR Green mix and primer pairs at 1 µM). All PCR reactions followed the same

protocol: 7 min at 95°C, 40 cycles of 10 s at 95°C, 10 s at 55°C and 30 s at 72°C. The specificity of the amplified product was confirmed for each primer pair using a melting curve. Data analysis was carried out with PikoReal software. Three biological replicates and two technical repetitions were performed for each sample. Relative transcript levels of the *LuPLR1* and CML15b (Lus10027243) genes were obtained using the specific primers qLuPLR1-F: 5'-TATGGAGATGGCAACGTCAA-3', qLuPLR1-R: 5'-TTGGTTGCCTGAGAGCTTTT-3', qCML15b-F: 5'-GGCAACGAGATACACGACCT-3' and qCML15bR: 5'-CCCTATCGAACAGCTGGAAG-3', designed with Primer3 software (Koressaar and Remm, 2007), and normalized using the comparative ΔΔCq method using two validated housekeeping reference genes selected by Huis *et al.*, 2010*b* (Huis et al., 2010): LuCYC encoding cyclophilin (using primers qLuCYC-F: 5'-TGATTGCGGTCAGCTGTAG-3' and qLuCYC-R: 5'AGGTGAAACGCTAGGCAGAA-3') and LuETIF5A encoding an Eukaryotic Translation Initiation Factor 5A (using primers qLuETIF5A-F: 5'-TGCCACATGTGAACCGTACT-3' and qLuETIF5A-R: 5'-CTTTACCCTCAGCAAATCCG-3').

2.8. Gene expression network

Putative coding sequences were searched through BLAST-P against the *L. usitatissimum* proteome available on Phytozome database. Public RNAseq data were downloaded from http://142.244.185.16/downloads/RNASeq/ and normalized using the geometric mean of cyclophilin *LuCYC* (*Lus10012167*) and the eukaryotic translation initiation factor 3H *LuETIF3H* (*Lus10007054*) gene expressions followed by $\log_2$ transformation. Visualization and data analysis were carried out with MeV 4.9.0 (Saeed et al., 2006). Hierarchical clustering was performed with the Pearson uncentered metric with the average linkage clustering method. The complete list of these genes and their Phytozome numbers is presented in Table S1. A gene expression correlation matrix was then constructed using pair-wise Pearson correlation coefficients (PCC). A co-expression network was visualized using Cytoscape 2.8.3 software representing only significant PCC values at $p < 0.05$ with a cut-off value of 0.95. Colors from yellow to red indicate increasing PCC values where the connection size indicates the strength of the connection.

2.9. Secoisolariciresinol extraction and HPLC analysis

The secoisolariciresinol extraction procedure described by Renouard et al. (2010) (Renouard et al., 2010) was adapted for lignan extraction from flax cell suspensions and immature seeds. Briefly, 500 mg of lyophilized cells were incubated with 20 ml of 80% (v/v) aqueous methanol, for 2 h at 60°C under stirring in a water bath. Following centrifugation, the solid residue was discarded and the supernatant was subsequently evaporated to dryness at 40°C and then resuspended in 1 ml of 0.1 M citrate-phosphate pH 4.8 buffer containing 5 units.ml^{-1} of ß-glucosidase from almonds (Sigma, St Quentin Fallavier, France) for secoisolariciresinol release during 4 h at 40°C. It was finally extracted twice with ethyl acetate, evaporated to dryness, resuspended in ethanol and filtered (0.45 µm, Millipore, Molsheim, France) before HPLC injection. The HPLC procedure was described in our previous work (Corbin et al., 2013a).

2.10. ABA extraction and quantification

The ABA extraction from whole seeds was based on the procedure of Agrawal et al. (2001) (Agrawal et al., 2001). Immature seeds (100 mg FW) were weighed, freeze-dried for 3 h, and extracted for 16 h at 4°C in the dark with MilliQ (Millipore, Molsheim, France) water (water/tissue ratio 50:1, v/w). ABA was quantified using a Phytodetek ABA ELISA kit (Agdia, Grigny, France) with (±) *cis–trans* ABA (Sigma, St Quentin Fallavier, France) as a standard.

2.11. Fluorescence imaging and estimation of cytosolic Ca^{2+}

The fluorescence imaging of the cells was recorded in the presence of 5 µM of Fluo 3-AM (Sigma), a Ca^{2+}-specific probe, according to the protocol described by Li et al. (2015). Cells placed in water on a glass slide with a cover slip were examined under light or fluorescence microscopy using an Olympus CX40 equipped with an Olympus U-RFLT50-200 laser (Olympus, Mannheim, Germany) using a 488 nm excitation filter and a 515-565 nm wavelength pass filter. Pictures were taken with an 8 megapixel eyesight camera (MD239 F/A). Image analysis was performed with ImageJ software (Abràmoff et al., 2004). The plot profile tool was used to quantify the fluorescence signal intensity in the cytoplasm.

2.12. Protein Kinase C activity

PKC activity was determined using the PepTag assay (Promega, Charbonières les Bains, France) according to the manufacturer's instructions. Briefly, a PKC-specific fluorescent

peptide was phosphorylated by the active PKCs of the cell lysate. The reaction mixture was 1 µl cell lysate, 0.4 mg/ml peptide, 100 mmol HEPES (pH 7.4), 6.5 mmol $CaCl_2$, 5 mmol dithiothreitol, 50 mmol $MgCl_2$, 5 mmol adenosine triphosphate, 10 µmol leupeptin and 1 mg/ml phosphatidylserine. Following 30 min of incubation at 37°C, phosphorylated and dephosphorylated peptide molecules were separated by 0.8% (50 mmol Tris-HCl, pH 8.0) agarose gel electrophoresis for 15 min at 100 V. The resulting bands were visualized under UV light.

2.13. Statistical analysis of the data

All data presented in this study are the means and standard deviations of at least three independent replicates (at least three independent biological replicates and two technical replicates, the number of independent biological replicates is indicated in each figure legend). Comparative statistical analyses of groups were performed using Student's t-test or one-way analysis of variance, according to the data.

3. Results

3.1. Cytosolic Ca^{2+} content is enhanced by ABA and displays a synergistic effect with ABA activation of LuPLR1 *gene expression*

In previous work (Corbin et al., 2013b, 2013a; Renouard et al., 2012b), we showed the positive role of ABA in *PLR1* gene expression. In order to evaluate whether cytosolic Ca^{2+} was involved in this regulation, increasing concentrations of ABA were applied on flax cell suspensions. The variation in the cytosolic Ca^{2+} level in response to ABA treatment was assessed using the Ca^{2+}-sensitive fluorescent dye, Fluo 3-AM. Cell imaging of intracellular fluorescence clearly indicated an increase in cytosolic Ca^{2+} in response to exogenous ABA (Fig. 1A-C). The ABA-mediated increase in cytosolic Ca^{2+} was dose-dependent, reaching a plateau at 100 µM (Fig. 1C). Interestingly, when cells were treated with elevated concentrations of ABA (i.e. 100 µM), fluorescent granules were clearly observed (Fig. 1A). These Ca^{2+} granules could either act as ion stores or constitute accumulation sites for detoxification as observed in other living organisms (Simkiss and Taylor, 1994).

Next, increasing concentrations of Ca^{2+} and ABA were applied on flax cell suspensions stably transformed with a construct containing the complete *LuPLR1* gene promoter fused to the *uidA* reporter gene. The resulting β-glucuronidase reporter gene activity values are presented in Fig. 2a. For each exogenous ABA concentration applied (ranging from 0 to 100 µM), the *LuPLR1* gene promoter activity was increased by the addition of Ca^{2+} with external exogenous concentrations ranging from 0 to 5 mM (Fig. 2A). Interestingly, while an increase in ABA concentration alone was sufficient to trigger a rise in *LuPLR1* promoter activity, an increase in Ca^{2+} concentration alone did not lead to any significant changes in *LuPLR1* gene expression (Fig. 2A). This effect of Ca^{2+} and ABA was confirmed by RT-qPCR analysis of *LuPLR1* gene expression in cells subjected to ABA treatment with different extracellular Ca^{2+} concentrations (Fig. 2B). Accordingly, the (+)-secoisolariciresinol accumulation, resulting from the LuPLR1 activity, was largely enhanced after Ca^{2+} addition in ABA-treated cells (Fig. 2C). On the contrary, for cells growing in Ca^{2+}-depleted medium, only a slight induction of lignan production was noted in response to exogenous ABA treatment (Fig. 2C), demonstrating the essential role of Ca^{2+} in this regulation.

3.2. ABA-mediated activation of LuPLR1 *gene expression is impaired by Ca^{2+} influx disruption*

In order to test whether the Ca^{2+} effect on *LuPLR1* expression activation was due only to a direct uptake from the extracellular Ca^{2+} or if Ca^{2+} intracellular stores, such as the vacuole, were also involved, the effect of a series of specific inhibitors was assessed. It should be noted that all the specific inhibitors used in the present study have been used in plants to modulate Ca^{2+} signaling (Angeles Sánchez-Sampedro et al., 2005; Dammann et al., 1997; Dubrovina et al., 2009; Hashimoto and Kudla, 2011; Zhao et al., 2011b, 2011a). The concentration of each compound was chosen to ensure that they exerted their maximal effects (inhibition or activation based on *LuPLR1* gene expression) without affecting cell growth (Fig. S1).

First, the modulatory effects of an extracellular Ca^{2+} chelator, EGTA, or a Ca^{2+} competitor, cadmium (Cd^{2+}), on the ABA-mediated transcriptional activation of the *LuPLR1* gene promoter were investigated using 100 µM ABA-treated flax cells cultured in incubation medium supplemented with 5 mM Ca^{2+} (Fig. 3). Following addition of Cd^{2+} or EGTA, *LuPLR1* promoter activity and (+)-secoisolariciresinol level decreased down to the level observed for untreated cells (Fig. 3A), evidencing a crucial role of Ca^{2+} influx in this metabolite pathway through the ABA-mediated transcriptional regulation of *LuPLR1* (Fig. 3B).

As Cd^{2+} could be toxic for cells, even at the concentration used here, more specific inhibitors were then tested to confirm this result. Nifedipine (NIF), an outer membrane channel blocker, was able to abolish the increase in cytosolic Ca^{2+} level in response to ABA addition (Fig. 4A-B), which reduced both the ABA effect on *LuPLR1* gene expression induction (Fig. 4C) and lignan accumulation (Fig. 4D), confirming the requirement of the Ca^{2+} influx for this ABA-related regulation. On the contrary, the use of heparin (HEP), an inhibitor of vacuolar Ca^{2+} release, had less impact on the increase of Ca^{2+} level in response to ABA (Fig. 4A-B), as well as on the activation of the *LuPLR1* promoter (Fig. 4C) and lignan accumulation (Fig. 4D). These results indicate that the Ca^{2+} flux mediating the ABA effect on *LuPLR1* gene expression originates more from the extracellular medium than from intracellular stores.

3.3. Ca^{2+} sensors CaM and CDPK are required for the ABA-mediated transcriptional activation of the **LuPLR1** *gene in cell suspension*

In order to decipher the Ca^{2+} transduction signaling involved in the *LuPLR1* gene promoter activation in response to an exogenous ABA supply, the respective involvement of the CaM- and/or CDPK-type Ca^{2+} sensors was investigated using their specific inhibitors: staurosporine (STAU), an antagonist of CDPKs, and calmidazolium (CALM), a potent inhibitor of CaMs.

The inhibition of CDPKs resulting from STAU treatment was first assessed by an in-gel kinase assay using a specific CDPK fluorescent substrate and total protein extracts prepared from flax cells (Fig. 5A). In cells treated with ABA, CDPK activity was detected and increased with protein concentration (Fig. 5A). On the contrary, STAU addition resulted in a dramatic decrease in the CDPK activity confirming its inhibitory action on these enzymes (Fig. 5A). As STAU could be toxic for plant cells, two different concentrations classically used in the literature were tested (i.e. 5 µM (Stau1) and 10 µM (Stau2), Fig. 5A). The lowest concentration of STAU was effective in inhibiting CDPK activity (Fig. 5A), so this concentration was used in subsequent experiments to limit the potential toxic and pleiotropic effects of this drug.

Application of 5 µM of STAU led to a significant decrease in the positive action of Ca^{2+} on the activation of *LuPLR1* promoter in response to ABA, supporting the involvement of CDPKs in this regulation (Fig. 5B). This transcriptional regulation resulted in a marked decrease in (+)-secoisolariciresinol accumulation (Fig. 5C).

Likewise, the effect of Ca^{2+} and ABA on the activity of *LuPLR1* promoter and lignan accumulation was abolished by CALM treatment (Fig. 5B-C), evidencing the critical role of CaMs as Ca^{2+} sensors in this ABA-driven regulation.

3.4. CaM and CDPK are also required for ABA control of lignan biosynthesis during flaxseed maturation

To assess the role of Ca^{2+} signaling in ABA-driven *LuPLR1* gene expression and (+)-secoisolariciresinol accumulation during seed maturation, we took advantage of a system previously used to elucidate lignan biosynthetic pathway and ABA regulation of this pathway in flax maturing seeds (Ford et al., 2001; Renouard et al., 2012b). Capsules containing immature flaxseeds (developmental stage 2, Fig. 6A; (Hano et al., 2006b)) were placed in wells of a 96-well microplate with peduncles soaking in solutions containing mock, ABA and/or Ca^{2+} signaling inhibitor (Fig. 6A). This treatment confirmed the up-regulation of *LuPLR1* gene expression (Fig. 6B), concomitantly with the increase in ABA concentration measured in flaxseed leading to a strong increase in the (+)-secoisolariciresinol net synthesis (Fig. 6C). Interestingly, even though a high ABA level remained in the seeds, application of STAU and CALM abolished the effect of high ABA concentration on *LuPLR1* gene expression and (+)-secoisolariciresinol synthesis (Fig. 6B-C), confirming that both CDPKs and CaMs-related are required for the control of ABA on the lignan biosynthesis in flaxseed.

3.5. Promoter cis*-acting elements are involved in the Ca^{2+} modulation of the ABA-mediated transcriptional activation of the* LuPLR1 *gene*

To investigate whether the two characterized ABA-responsive *cis*-acting elements of the *LuPLR1* promoter, ABRE and MYB2 (Corbin et al., 2013b; Renouard et al., 2012a), were involved in the Ca^{2+} modulation of *LuPLR1* expression, the consequences of mutations on single or both elements were analyzed (Fig. 7A). β-glucuronidase activities of transiently transformed flax cell suspensions treated with ABA and Ca^{2+} in the presence of different inhibitors were monitored (Fig. 7B). Both elements are involved in the Ca^{2+}-dependent ABA response of *LuPLR1* gene expression since their single disruption resulted in the complete loss of the additive effect of Ca^{2+} on the ABA regulation of this gene (Fig. 7B). The simultaneous disruption of the ABRE and MYB2 patterns suppressed the positive Ca^{2+} effect on the ABA-mediated transcriptional activation of *LuPLR1* and no further effect was observed for additional inhibitor treatment (Fig. 7B) indicating that these two elements are required and sufficient to confer transcriptional regulation of the *LuPLR1* gene in response to the ABA-mediated cytosolic Ca^{2+} increase. The *LuPLR1* promoter activity resulting from the mutation of the sole ABRE element (Fig. 7A) was greatly affected by HEP and to a lesser extent by CALM (Fig. 7B). On the contrary, stronger inhibition effects resulting from STAU, NIF and HEP treatments were measured (Fig. 7B) with the mutation of the sole MYB2 motif (Fig. 7A).

3.6. Identification and characterization of CML15b as a key regulator for the Ca^{2+}-dependent ABA activation of SDG biosynthesis

To gain further insight into the identification of potential regulators, a global search for protein domains of calcium sensors such as CaM, CML or CDPK was carried out within the flax deduced proteome (Wang et al., 2012), available on the Phytozome database (Goodstein et al., 2012), using BLOSUM62 as comparison matrix at the score value of > 300 and e-value < e^{-100}. The PFAM, PANTHER and KEGG domains used for this search are mentioned on Table S1, and the retrieved gene encoding for the corresponding proteins from flax were named according to their closest orthologs from *Arabidopsis thaliana*. Then, their relative expression profiles during flax seed development were extracted from RNAseq public datasets for flax (Fenart et al., 2010; Kumar et al., 2013) normalized and presented using the MeV suite (Saeed et al., 2006). Results including the expression profiles of *LuDIR5*, *LuPLR1*

and *LuUGT74S1* (Corbin et al., 2018; Dalisay et al., 2015; Fofana et al., 2017; Renouard et al., 2014), the 3 biochemically and functionally characterized genes involved in SDG biosynthesis, are depicted in Fig. S2. From these data a co-expression network with candidates potentially involved in Ca^{2+} signaling and the lignan biosynthetic genes *LuDIR5*, *LuPLR1* and *LuUGT74S1* was generated using Cytoscape software with a cut-off value of 0.95 at a *p*-value < 0.05 (Kumar et al., 2013). From this analysis, 18 candidates appeared significantly correlated with *LuPLR1* (6 CMLs (*CML15b*, *CML15d*, *CML18b*, *CML30f*, *CML30g* and *CML42b*), 4 CDPKs (*CDPK14c*, *CDPK17a*, *CDPK24a* and *CDPK24b*) as well as 6 others CBPs (Ca^{2+}-binding proteins: *CBP2*, *CBP11*, *CBP15*, *CBP16*, *CBP17* and *CBP18*) and 2 IQs (isoleucine glutamine) domain containing proteins (*IQ3a* and *IQ12*) (Figure 8a). Among them 6 were significantly linked with *LuDIR5* (*CML15b*, *CML30g*, *CBP11*, *CBP15*, *IQ3a* and *IQ12*) whereas only 3 were linked with *LuUGT74S1* (*CML15b*, *CBP11* and *IQ3a*) (Fig. 8A, Table S2). Considering its expression profile depicted in Fig. 8B and the key role of CaM and CML highlighted by the aforementioned results from this study, we decided to focus on the role of CML15b. To provide direct *in vivo* evidence for the possible involvement of CML15b in the regulation of the Ca^{2+}-dependent ABA activation of SDG biosynthesis we generated an RNAi construct (Fig. 8C). For this purpose, the target sequence was designed using the pssRNAit server tool dedicated to the design of effective and specific (limiting off-target silencing) and non-toxic siRNAs for plant RNAi (Dai and Zhao, 2011). The T-DNA was transferred in flax cells using transient *A. tumefaciens*-mediated transformation. The efficiency of the transformation was asserted by the visualization of the *E-GFP* expression under fluorescence microscopy observation of the flax cells as shown in Fig. 8D. As expected, a significant decrease in *CML15b* gene expression was detected by RT-qPCR in transformed cells (*iCML15b*, Fig. 8E) - both untreated and ABA-treated in presence of 5 mM exogenous Ca^{2+}, as compared to untransformed cells (WT, Fig. 8E). We also noted that this ABA-treatment led to an increase in *CML15b* gene expression (Fig. 8E). This RNAi approach also had a significant impact on *LuPLR1* gene expression by significantly decreasing its activation by ABA treatment (Fig. 8F). This trend was confirmed at metabolic level by a significant decrease of (+)-secoisolariciresinol accumulation in response to ABA treatment in the transgenic cells (Fig. 8G). Taken together, these results revealed a strong and significant impact of *CML15b* gene expression disruption on the Ca^{2+}-dependent ABA activation of *LuPLR1* gene expression and SDG biosynthesis, thus providing direct *in vivo* evidence for the involvement of CML15b.

458

459 ***3.7. Proposed model***

460 Overall, these results demonstrate a crucial role for Ca^{2+} as a mediator of the ABA control of
461 lignan biosynthesis through the transcriptional regulation of the *LuPLR1* gene and provide the
462 outline for a gene regulatory mechanism described in Fig. 9. Upon perception, ABA triggers
463 an increase in the cytosolic Ca^{2+} concentration originating mainly from the extracellular
464 compartment, although the intracellular stores also seem to participate in the transcriptional
465 activation specifically through the MYB2 binding element. The Ca^{2+} signal is then relayed by
466 CaM and CDPK, which modulate ABA signaling through activation of transcription factors
467 (TFs) such as MYB, ABF or bZIP either by a phosphorylation cascade or a direct interaction.
468 As a final point, these TF act specifically on the ABRE and MYB2 boxes of the *LuPLR1* gene
469 promoter, activating its gene expression and thereby lignan biosynthesis. The present results
470 support a more likely activation of the ABRE *cis*-acting element through the action of CDPK-
471 dependent TF whereas the MYB2 binding site was found to be more sensitive to the
472 disruption of the CaM action. A key role of LuCML15b is here proposed in this regulation.

473

4. Discussion

Application of Ca^{2+} inhibitors, chelators or competitors, affecting the Ca^{2+} level and/or availability, evidenced a critical role for Ca^{2+} concentration and availability in the ABA-mediated lignan biosynthesis regulation through transcriptional activation of the *LuPLR1* gene. Ca^{2+} is a well-known second messenger of ABA signaling which have been described to trigger Ca^{2+} release into the cytosol from extracellular medium and/or intracellular stores (Lecourieux et al., 2006). This action of ABA on the control of cytosolic Ca^{2+} movements may explain why Ca^{2+} alone was not able to increase *LuPLR1* gene expression nor SDG accumulation. The inhibition observed in our experiments when using EGTA or Cd^{2+} showed the importance of Ca^{2+} as a modulator of the ABA action in the context of lignan biosynthesis in flax and revealed that the rise in cytosolic Ca^{2+} in response to exogenous ABA was due to an increased Ca^{2+} influx. Such a specificity of intra- *vs* extra-cellular Ca^{2+} origin has been observed in *Silybum marianum* cell suspensions (Angeles Sánchez-Sampedro et al., 2005). Changes in intracellular Ca^{2+} concentration have to be detected in order to produce the correct cascade of events, such as protein phosphorylation or gene expression reprogramming (Hashimoto and Kudla, 2011). For this purpose, plants display an extensive and complex array of specific sensors decoding Ca^{2+} concentration variations. These include CaM and/or CaM-like proteins as well as CDPK and their interacting kinases, which represent specific, robust and flexible information processing sensors for the correct signal transduction as observed for ABA signaling (Zhao et al., 2011a, 2011b). In potato, ABA-inducible wounding genes were inhibited by STAU application resulting in an effective inhibition of CDPKs (Dammann et al., 1997). In our experiments, CALM and STAU inhibitors of Ca^{2+} transduction prevented the induction of *LuPLR1* expression by ABA, thus suggesting a key role for both CaMs and CDPKs as Ca^{2+} sensors modulating ABA signaling.

In the regulation of the biosynthesis of phenylpropanoid-derived products, Ca^{2+} was shown to enhance the production of flavonolignans in an elicited cell culture of *S. marianum* (Angeles Sánchez-Sampedro et al., 2005). More recently, Ca^{2+} and ABA interplay have been evidenced in the accumulation regulation of total phenolics and anthocyanins in grape cell suspension (Martins et al., 2018). In *Vitis amurensis* cultures, CDPKs are essential for the production of resveratrol (Dubrovina et al., 2009). CMLs have been shown to positively regulate the expression of flavonoids biosynthetic genes in grape (Gollop et al., 2002; Vitrac et al., 2000). Foliar application of Ca^{2+} enhanced both the expression of anthocyanin biosynthetic genes as well as anthocyanin accumulation in strawberry fruits (Xu et al., 2014) through CaM/CML

actions (Peng et al., 2016). Here, direct evidences for the role of CML15b in the regulation of lignan biosynthesis in response to ABA in flax were provided by RNAi experiments and confirmed the key role of this gene family in the control of secondary metabolites accumulation.

We have previously demonstrated the roles of the ABRE and MYB2 cis-acting elements in the ABA-mediated regulation of lignan biosynthesis through the transcriptional control of the *LuPLR1* gene (Corbin et al., 2013a). Here, the effects of mutations of these two elements in the *LuPLR1* gene promoter support a function as Ca^{2+}-sensitive sequences involved in this ABA-mediated regulation. ABRE and MYB2 binding sites are very common in the promoters of ABA-regulated genes (Abe et al., 2003; Finkelstein et al., 2002; Gutierrez et al., 2007) and the ABRE-related sequences constitute well known Ca^{2+}-responsive *cis*-acting elements (Kaplan et al., 2006; Whalley et al., 2011). CDPKs have been shown to phosphorylate the ABA-responsive TFs, ABFs (ABRE-Binding Factors), which are important mediators of ABA-mediated signaling (Choi et al., 2005; Zhu et al., 2007).
Furthermore, the MYB2 transcription factor possesses a binding domain for CaM proteins and its DNA binding capacity is regulated in a Ca^{2+}-dependent manner (Yoo et al., 2005). CaMs may control CDPKs phosphorylating target transcription factors, both having consequences on the regulation of transcription (Reddy, 2001). Future works will be conducted to elucidate the complete molecular mechanism of this regulation.

5. Conclusions

To conclude, the results described herein demonstrate a crucial role for Ca^{2+} signaling in the ABA-positive regulation of lignan biosynthesis through the transcriptional control of the *LuPLR1* gene and allow the identification of CML15b as a key mediator of this regulation. This regulation was conserved in both systems studied: cell suspensions and maturing seeds. Taken together, these results provide important new information on the regulation of lignans biosynthesis. These results could help with the design of future biotechnological approaches directed toward *in planta* lignans production for broad ranges of possible applications since these compounds are involved in both plant defense and human health-promotion. Indeed the present results clearly demonstrate that *L. usitatissimum* cell suspension elicited by both ABA and Ca^{2+} could be an attractive renewable system for the production of SDG.

Declarations of interest

None

Acknowledgements

This work was financially supported by the "Ligue contre le Cancer, Comité d'Eure et Loir". LM received a PhD grant from the "Ministère de Enseignement Supérieur et Recherche". CC received a PhD grant from the "Conseil Régional Centre-Val de Loire". The authors thank Carol Robins (Scientific English) for English editing.

Author contributions LM, CC, SD, LGa, CD, SR, TL and GM performed the research. CH, DA, LGu and EL designed the research. CH, LGu and EL analyzed the data. CH wrote the manuscript. All the authors edited and then approved the final version of this manuscript.

List of abbreviations:

ABF: ABRE Binding Factor; ABI3: ABA Insensitive 3; ABRE: ABA Response Element; b-ZIP: Leucine Zipper factor; Ca^{2+}: Calcium; CALM: Calmidazolium; CAM: Calmodulin; CML: Calmodulin-like; Cd^{2+}: Cadmium; CDPK: Calcium-Dependent Protein Kinase; Cq: Quantification cycle; CTL: Control; cv: cultivar; CYC: Cyclophilin; DMSO: Dimethylsulfoxide; EGTA: Ethylene Glycol Tetra-acetic Acid; ER: Endoplasmic Reticulum; ERA1: Enhanced Response to ABA 1; ETIF5A: Eukaryotic Translation Initiation Factor 5A; GUS: β-Glucuronidase; HEP: Heparine; InsP3: Inositol Triphosphate; MS: Murashige and Skoog; MU: 4-methylumbelliferone; MUG: 4-methylumbelliferyl-β-D-glucuronide; MYB: Myeloblastosis-derived transcription factor; NIF: Nifedipine; PCV: Packed Cell Volume; PLR: Pinoresinol Lariciresinol Reductase; RFU: Relative Fluorescence Unit; ROS: Reactive Oxygen Species; RT: Reverse Transcription; STAU: Staurosporine; TF: Transcription Factor; uidA: β-Glucuronidase encoding gene.

567 **References**

568 Abe, H., Urao, T., Ito, T., Seki, M., Shinozaki, K., 2003. Arabidopsis AtMYC2 (bHLH) and
569 AtMYB2 (MYB) Function as Transcriptional Activators in Abscisic Acid Signaling.
570 Plant Cell 15, 63–78. https://doi.org/10.1105/tpc.006130.salt
571 Abràmoff, M.D., Hospitals, I., Magalhães, P.J., Abràmoff, M., 2004. Image Processing with
572 ImageJ. Biophotonics Int. 11, 36–42.
573 Agrawal, G.K., Yamazaki, M., Kobayashi, M., Hirochika, R., Miyao, A., Hirochika, H., 2001.
574 Screening of the Rice Viviparous Mutants Generated by Endogenous Retrotransposon
575 Tos17 Insertion. Tagging of a Zeaxanthin Epoxidase Gene and a Novel OsTATC Gene.
576 Plant Physiol. 125, 1248–1257. https://doi.org/10.1104/pp.125.3.1248
577 Angeles Sánchez-Sampedro, M., Fernández-Tárrago, J., Corchete, P., 2005. Enhanced
578 silymarin accumulation is related to calcium deprivation in cell suspension cultures of
579 Silybum marianum (L.) Gaertn. J. Plant Physiol. 162, 1177–82.
580 https://doi.org/10.1016/j.jplph.2005.01.012
581 Arimura, G.-I., Maffei, M.E., 2010. Calcium and secondary CPK signaling in plants in
582 response to herbivore attack. Biochem. Biophys. Res. Commun. 400, 455–60.
583 https://doi.org/10.1016/j.bbrc.2010.08.134
584 Batistič, O., Kudla, J., 2012. Analysis of calcium signaling pathways in plants. Biochim.
585 Biophys. Acta 1820, 1283–93. https://doi.org/10.1016/j.bbagen.2011.10.012
586 Berger, B., Stracke, R., Yatusevich, R., Weisshaar, B., Flügge, U.-I., Gigolashvili, T., 2007. A
587 simplified method for the analysis of transcription factor-promoter interactions that
588 allows high-throughput data generation. Plant J. cell Mol. Biol. 50, 911–6.
589 https://doi.org/10.1111/j.1365-313X.2007.03088.x
590 Busk, P.K., Pagès, M., 1998. Regulation of abscisic acid-induced transcription. Plant Mol.
591 Biol. 37, 425–35.
592 Choi, H., Park, H., Park, J.H., Kim, S., Im, M., Seo, H., Kim, Y., Hwang, I., Kim, S.Y., 2005.
593 Arabidopsis Calcium-Dependent Protein Kinase AtCPK32 Interacts with ABF4 , a
594 Transcriptional Regulator of Abscisic Acid-Responsive Gene Expression , and
595 Modulates Its Activity 1. Plant Physiol. 139, 1750–1761.
596 https://doi.org/10.1104/pp.105.069757.by
597 Corbin, C., Decourtil, C., Marosevic, D., Bailly, M., Lopez, T., Renouard, S., Doussot, J.,
598 Dutilleul, C., Auguin, D., Giglioli-Guivarc'h, N., Lainé, E., Lamblin, F., Hano, C.,
599 2013a. Role of protein farnesylation events in the ABA-mediated regulation of the

Pinoresinol-Lariciresinol Reductase 1 (LuPLR1) gene expression and lignan biosynthesis in flax (Linum usitatissimum L.). Plant Physiol. Biochem. 72, 96–111. https://doi.org/10.1016/j.plaphy.2013.06.001

Corbin, C., Drouet, S., Markulin, L., Auguin, D., Lainé, É., Davin, L.B.L.B., Cort, J.R.J.R., Lewis, N.G.N.G., Hano, C., 2018. A genome-wide analysis of the flax (Linum usitatissimum L .) dirigent protein family: from gene identification and evolution to differential regulation. Plant Mol. Biol. 97, 73–101. https://doi.org/10.1007/s11103-018-0725-x

Corbin, C., Drouet, S., Mateljak, I., Markulin, L., Decourtil, C., Renouard, S., Lopez, T., Doussot, J., Lamblin, F., Auguin, D., Lainé, E., Fuss, E., Hano, C., 2017. Functional characterization of the pinoresinol–lariciresinol reductase-2 gene reveals its roles in yatein biosynthesis and flax defense response. Planta 246, 1–16. https://doi.org/10.1007/s00425-017-2701-0

Corbin, C., Renouard, S., Lopez, T., Lamblin, F., Lainé, E., Hano, C., 2013b. Identification and characterization of cis-acting elements involved in the regulation of ABA- and/or GA-mediated LuPLR1 gene expression and lignan biosynthesis in flax (Linum usitatissimum L.) cell cultures. J. Plant Physiol. 170, 516–522. https://doi.org/10.1016/j.jplph.2012.11.003

Dai, X., Zhao, P.X., 2011. PsRNATarget: A plant small RNA target analysis server. Nucleic Acids Res. 39, 155–159. https://doi.org/10.1093/nar/gkr319

Dalisay, D.S., Kim, K.W., Lee, C., Yang, H., Rübel, O., Bowen, B.P., Davin, L.B., Lewis, N.G., 2015. Dirigent Protein-Mediated Lignan and Cyanogenic Glucoside Formation in Flax Seed: Integrated Omics and MALDI Mass Spectrometry Imaging. J. Nat. Prod. 78, 1231–1242. https://doi.org/10.1021/acs.jnatprod.5b00023

Dammann, C., Rojo, E., Sanchez-Serrano, J.J., 1997. Abscisic acid and jasmonic acid activate wound inducible genes in potato through separate, organ specific signal transduction pathways. Plant J. 11, 773–782.

Dubrovina, A.S., Kiselev, K. V, Veselova, M. V, Isaeva, G.A., Fedoreyev, S.A., Zhuravlev, Y.N., 2009. Enhanced resveratrol accumulation in rolB transgenic cultures of Vitis amurensis correlates with unusual changes in CDPK gene expression. J. Plant Physiol. 166, 1194–206. https://doi.org/10.1016/j.jplph.2009.01.006

Fenart, S., Ndong, Y.-P., Duarte, J., Rivière, N., Wilmer, J., van Wuytswinkel, O., Lucau, A., Cariou, E., Neutelings, G., Gutierrez, L., Chabbert, B., Guillot, X., Tavernier, R.,

633 Hawkins, S., Thomasset, B., 2010. Development and validation of a flax (Linum
634 usitatissimum L.) gene expression oligo microarray. BMC Genomics 11, 592.
635 https://doi.org/10.1186/1471-2164-11-592
636 Finkelstein, R.R., Gampala, S.S.L., Rock, C.D., 2002. Abscisic Acid Signaling in Seeds and
637 Seedlings. Plant Cell S15-45. https://doi.org/10.1105/tpc.010441.would
638 Fofana, B., Ghose, K., McCallum, J., You, F.M., Cloutier, S., 2017. UGT74S1 is the key
639 player in controlling secoisolariciresinol diglucoside (SDG) formation in flax. BMC
640 Plant Biol. 17, 1–13. https://doi.org/10.1186/s12870-017-0982-x
641 Ford, J.D., Huang, K., Wang, H., Davin, L.B., Lewis, N.G., 2001. Biosynthetic Pathway to
642 the Cancer Chemopreventive Secoisolariciresinol Diglucoside - Hydroxymethyl Glutaryl
643 Ester-Linked Lignan Oligomers in Flax (Linum usitatissimum) Seed † 2, 1388–1397.
644 Frey, A., Godin, B., Bonnet, M., Sotta, B., Marion-Poll, A., 2004. Maternal synthesis of
645 abscisic acid controls seed development and yield in Nicotiana plumbaginifolia. Planta
646 218, 958–64. https://doi.org/10.1007/s00425-003-1180-7
647 Gang, D.R., Kasahara, H., Xia, Z.Q., Mijnsbrugge, K. Vander, Bauw, G., Boerjan, W., Van
648 Montagu, M., Davin, L.B., Lewis, N.G., 1999. Evolution of plant defense mechanisms:
649 Relationships of phenylcoumaran benzylic ether reductases to pinoresinol-lariciresinol
650 and isoflavone reductases. J. Biol. Chem. 274, 7516–7527.
651 https://doi.org/10.1074/jbc.274.11.7516
652 Gollop, R., Even, S., Colova-Tsolova, V., Perl, A., 2002. Expression of the grape
653 dihydroflavonol reductase gene and analysis of its promoter region. J. Exp. Bot. 53,
654 1397–1409. https://doi.org/10.1093/jexbot/53.373.1397
655 Goodstein, D.M., Shu, S., Howson, R., Neupane, R., Hayes, R.D., Fazo, J., Mitros, T., Dirks,
656 W., Hellsten, U., Putnam, N., Rokhsar, D.S., 2012. Phytozome: a comparative platform
657 for green plant genomics. Nucleic Acids Res. 40, D1178--86.
658 https://doi.org/10.1093/nar/gkr944
659 Gutierrez, L., Van Wuytswinkel, O., Castelain, M., Bellini, C., 2007. Combined networks
660 regulating seed maturation. Trends Plant Sci. 12, 294–300.
661 https://doi.org/10.1016/j.tplants.2007.06.003
662 Hano, C., Addi, M., Bensaddek, L., Crônier, D., Baltora-Rosset, S., Doussot, J., Maury, S.,
663 Mesnard, F., Chabbert, B., Hawkins, S., Lain??, E., Lamblin, F., Lainé, E., Lamblin, F.,
664 2006a. Differential accumulation of monolignol-derived compounds in elicited flax
665 (Linum usitatissimum) cell suspension cultures. Planta 223, 975–989.

https://doi.org/10.1007/s00425-005-0156-1

Hano, C., Martin, I., Fliniaux, O., Legrand, B., Gutierrez, L., Arroo, R.R.J., Mesnard, F., Lamblin, F., Lainé, E., 2006b. Pinoresinol-lariciresinol reductase gene expression and secoisolariciresinol diglucoside accumulation in developing flax (Linum usitatissimum) seeds. Planta 224, 1291–1301. https://doi.org/10.1007/s00425-006-0308-y

Hano, C., Renouard, S., Molinié, R., Corbin, C., Barakzoy, E., Doussot, J., Lamblin, F., Lainé, E., 2013. Flaxseed (Linum usitatissimum L.) extract as well as (+)-secoisolariciresinol diglucoside and its mammalian derivatives are potent inhibitors of $α$-amylase activity. Bioorg. Med. Chem. Lett. 23, 3007–3012. https://doi.org/10.1016/j.bmcl.2013.03.029

Hashimoto, K., Kudla, J., 2011. Calcium decoding mechanisms in plants. Biochimie 93, 2054–9. https://doi.org/10.1016/j.biochi.2011.05.019

Hepler, P.K., 2005. Calcium: a central regulator of plant growth and development. Plant Cell 17, 2142–55. https://doi.org/10.1105/tpc.105.032508

Huis, R., Hawkins, S., Neutelings, G., 2010. Selection of reference genes for quantitative gene expression normalization in flax (Linum usitatissimum L.). BMC Plant Biol. 10, 71. https://doi.org/10.1186/1471-2229-10-71

Kaplan, B., Davydov, O., Knight, H., Galon, Y., Knight, M.R., Fluhr, R., Fromm, H., 2006. Rapid transcriptome changes induced by cytosolic Ca2+ transients reveal ABRE-related sequences as Ca2+-responsive cis elements in Arabidopsis. Plant Cell 18, 2733–48. https://doi.org/10.1105/tpc.106.042713

Karimi, M., Inze, D., Depicker, A., 2002. GATEWAY vectors for Agrobacterium-mediated plant transformation. Trends Plant Sci. 7, 193–195. https://doi.org/10.1016/S1360-1385(02)02251-3

Koressaar, T., Remm, M., 2007. Enhancements and modifications of primer design program Primer3. Bioinformatics 23, 1289–91. https://doi.org/10.1093/bioinformatics/btm091

Kumar, S., Jordan, M.C., Datla, R., Cloutier, S., 2013. The LuWD40-1 Gene Encoding WD Repeat Protein Regulates Growth and Pollen Viability in Flax (Linum Usitatissimum L.). PLoS One 8, 1–10. https://doi.org/10.1371/journal.pone.0069124

Lainé, E., Hano, C., Lamblin, F.F., 2009. Phytoestrogens: Lignans, WILEY-VCH. ed. Weinheim.

Lecourieux, D., Ranjeva, R., Pugin, A., 2006. Calcium in plant defence-signalling pathways. New Phytol. 171, 249–69. https://doi.org/10.1111/j.1469-8137.2006.01777.x

699 Li, L., Lin, F., Qu, Y. and Zhang, Q., 2015. A Protocol to Measure the Cytoplasmic Calcium
700 in *Arabidopsis* Guard Cells. *Bio-protocol* 5(9): e1462.
701 https://doi.org/10.21769/BioProtoc.1462
702 Martins, V., Garcia, A., Costa, C., Sottomayor, M., Gerós, H., 2018. Calcium- and hormone-
703 driven regulation of secondary metabolism and cell wall enzymes in grape berry cells. J.
704 Plant Physiol. 231, 57–67. https://doi.org/10.1016/j.jplph.2018.08.011
705 Murashige, T., Skoog, F., 1962. A Revised Medium for Rapid Growth and Bio Assays with
706 Tobacco Tissue Cultures. Physiol. Plant. 15, 473–497. https://doi.org/10.1111/j.1399-
707 3054.1962.tb08052.x
708 Oomah, B.D., 2001. Flaxseed as a functional food source. J. Sci. Food Agric. 81, 889–894.
709 Peng, H., Yang, T., Whitaker, B.D., Shangguan, L., Fang, J., 2016. Calcium/calmodulin
710 alleviates substrate inhibition in a strawberry UDP-glucosyltransferase involved in fruit
711 anthocyanin biosynthesis. BMC Plant Biol. 16, 1–11. https://doi.org/10.1186/s12870-
712 016-0888-z
713 Pottosin, I.I., Schönknecht, G., 2007. Vacuolar calcium channels. J. Exp. Bot. 58, 1559–1569.
714 https://doi.org/10.1093/jxb/erm035
715 Reddy, A.S.N., 2001. Calcium: silver bullet in signaling. Plant Sci. 160, 381–404.
716 Reddy, A.S.N., Ali, G.S., Celesnik, H., Day, I.S., 2011. Coping with stresses: roles of
717 calcium- and calcium/calmodulin-regulated gene expression. Plant Cell 23, 2010–32.
718 https://doi.org/10.1105/tpc.111.084988
719 Renouard, S., Corbin, C., Lopez, T., Montguillon, J., Gutierrez, L., Lamblin, F., Lainé, E.,
720 Hano, C., 2012a. Abscisic acid regulates pinoresinol-lariciresinol reductase gene
721 expression and secoisolariciresinol accumulation in developing flax (Linum
722 usitatissimum L.) seeds. Planta 235, 85–98. https://doi.org/10.1007/s00425-011-1492-y
723 Renouard, S., Corbin, C., Lopez, T., Montguillon, J., Gutierrez, L., Lamblin, F., Lainé, E.,
724 Hano, C., Cyrielle, @bullet, @bullet, C., Lopez, T., Montguillon, J., Gutierrez, L.,
725 Frédéric, @bullet, @bullet, L., Lainé, E., Hano, C., 2012b. Abscisic acid regulates
726 pinoresinol–lariciresinol reductase gene expression and secoisolariciresinol accumulation
727 in developing flax (Linum usitatissimum L.) seeds. Planta 235, 85–98.
728 https://doi.org/10.1007/s00425-011-1492-y
729 Renouard, S., Hano, C., Corbin, C., Fliniaux, O., Lopez, T., Montguillon, J., Barakzoy, E.,
730 Mesnard, F., Lamblin, F., Lainé, E., 2010. Cellulase-assisted release of
731 secoisolariciresinol from extracts of flax (Linum usitatissimum) hulls and whole seeds.

Food Chem. 122, 679–687. https://doi.org/10.1016/j.foodchem.2010.03.036

Renouard, S., Tribalatc, M., Lamblin, F., Mongelard, G., Fliniaux, O., Corbin, C., Marosevic, D., Pilard, S., Demailly, H., Gutierrez, L., Hano, C., Lainé, E., 2014. RNAi-mediated pinoresinol lariciresinol reductase gene silencing in flax (Linum usitatissimum L .) seed coat : Consequences on lignans and neolignans accumulation. J. Plant Physiol. 171, 1372–1377. https://doi.org/10.1016/j.jplph.2014.06.005

Saeed, A.I., Bhagabati, N.K., Braisted, J.C., Liang, W., Sharov, V., Howe, E.A., Li, J., Thiagarajan, M., White, J.A., Quackenbush, J., 2006. TM4 microarray software suite. Methods Enzymol. 411, 134–93. https://doi.org/10.1016/S0076-6879(06)11009-5

Simkiss, K., Taylor, M.G., 1994. Calcium magnesium phosphate granules: atomistic simulations explaining cell death. J Exp Biol 190, 131–139.

Tuteja, N., 2009. Integrated Calcium Signaling in Plants, in: Mancuso, S., Baluska, F. (Eds.), Signaling in Plants, Signaling and Communication in Plants. Springer Berlin Heidelberg, Berlin, Heidelberg, pp. 29–50. https://doi.org/10.1007/978-3-540-89228-1

Tuteja, N., Mahajan, S., 2007. Calcium Signaling Network in Plants. Plant Signal. Behav. 2, 79–85.

Vitrac, X., Larronde, F., Krisa, S., Decendit, A., Deffieux, G., Merillon, J.-M., 2000. Sugar sensing and Ca2+ calmodulin requirement in Vitis vinifera cells producing anthocyanins. Phytochemistry 53, 659–665. https://doi.org/10.1016/S0031-9422(99)00620-2

Wang, Z., Hobson, N., Galindo, L., Zhu, S., Shi, D., McDill, J., Yang, L., Hawkins, S., Neutelings, G., Datla, R., Lambert, G., Galbraith, D.W., Grassa, C.J., Geraldes, A., Cronk, Q.C., Cullis, C., Dash, P.K., Kumar, P. a, Cloutier, S., Sharpe, A.G., Wong, G.K.-S., Wang, J., Deyholos, M.K., 2012. The genome of flax (Linum usitatissimum) assembled de novo from short shotgun sequence reads. Plant J. 72, 461–473. https://doi.org/10.1111/j.1365-313X.2012.05093.x

Westcott, N.D., Muir, A.D., 2003. Flax seed lignan in disease prevention and health promotion. Phytochem. Rev. 2, 401–417. https://doi.org/10.1023/B:PHYT.0000046174.97809.b6

Whalley, H.J., Sargeant, A.W., Steele, J.F.C., Lacoere, T., Lamb, R., Saunders, N.J., Knight, H., Knight, M.R., 2011. Transcriptomic analysis reveals calcium regulation of specific promoter motifs in Arabidopsis. Plant Cell 23, 4079–95. https://doi.org/10.1105/tpc.111.090480

White, P.J., Broadley, M.R., 2003. Calcium in plants. Ann. Bot. 92, 487–511.

765 https://doi.org/10.1093/aob/mcg164
766 Xu, F., Cao, S., Shi, L., Chen, W., Su, X., Yang, Z., 2014. Blue light irradiation affects
767 anthocyanin content and enzyme activities involved in postharvest strawberry fruit. J.
768 Agric. Food Chem. 62, 4778–4783. https://doi.org/10.1021/jf501120u
769 Yoo, J.H., Park, C.Y., Kim, J.C., Heo, W. Do, Cheong, M.S., Park, H.C., Kim, M.C., Moon,
770 B.C., Choi, M.S., Kang, Y.H., Lee, J.H., Kim, H.S., Lee, S.M., Yoon, H.W., Lim, C.O.,
771 Yun, D.-J., Lee, S.Y., Chung, W.S., Cho, M.J., 2005. Direct interaction of a divergent
772 CaM isoform and the transcription factor, MYB2, enhances salt tolerance in arabidopsis.
773 J. Biol. Chem. 280, 3697–706. https://doi.org/10.1074/jbc.M408237200
774 Zhao, R., Sun, H.-L., Mei, C., Wang, X.-J., Yan, L., Liu, R., Zhang, X.-F., Wang, X.-F.,
775 Zhang, D.-P., 2011a. The Arabidopsis Ca(2+) -dependent protein kinase CPK12
776 negatively regulates abscisic acid signaling in seed germination and post-germination
777 growth. New Phytol. 192, 61–73. https://doi.org/10.1111/j.1469-8137.2011.03793.x
778 Zhao, R., Wang, X.-F., Zhang, D.-P., 2011b. CPK12: A Ca2+-dependent protein kinase
779 balancer in abscisic acid signaling. Plant Signal. Behav. 6, 1687–90.
780 https://doi.org/10.4161/psb.6.11.17954
781 Zhu, S.-Y., Yu, X.-C., Wang, X.-J., Zhao, R., Li, Y., Fan, R.-C., Shang, Y., Du, S.-Y., Wang,
782 X.-F., Wu, F.-Q., Xu, Y.-H., Zhang, X.-Y., Zhang, D.-P., 2007. Two calcium-dependent
783 protein kinases, CPK4 and CPK11, regulate abscisic acid signal transduction in
784 Arabidopsis. Plant Cell 19, 3019–36. https://doi.org/10.1105/tpc.107.050666
785
786

Figure legends

Figure 1. Quantification of cytosolic Ca^{2+} in flax cell after ABA treatment

A. Cell imaging of intracellular fluorescence of the Fluo 3-AM Ca^{2+} probe in response to exogenous ABA supply. Flax cell suspensions were observed 24 h after probe addition and/or ABA supplementation under fluorescent (odd numbers) or visible (even numbers) light. Three controls were used: without probe or ABA supply but only DMSO addition (A1/A2); 50 µM ABA treatment (A3/A4) or probe addition (A5/A6). ABA concentrations: 10 µM in A7 and A8, 25 µM in A9 and A10 and 50 µM in A11 and A12.

B. Cell imaging of intracellular fluorescence of the Ca^{2+} probe Fluo 3-AM after 24 h of 100 µM exogenous ABA supply in flax cell suspensions under fluorescent (B1) or visible (B2) light and merged (B3). Arrows indicate granules.

C. Relative Fluorescence Units (RFUs) of flax cells in response to increasing ABA concentrations corresponding to the relative cytosolic Ca^{2+} concentration determined using a fluorometer after 24 h of treatment.

Data are expressed as the mean of 3 independent experimentations ± standard deviation of the mean and different letters indicate significant differences between conditions ($P < 0.05$).

(Color online).

Figure 2. Effect of different combined Ca^{2+} and ABA treatments on *LuPLR1* gene expression and (+)-secoisolariciresinol production in flax cells

A. The β-glucuronidase reporter activity of stably transformed flax cell suspensions was determined 48 h after an exogenous supply of ABA (from 0 to 100 µM). Data are expressed as the mean (n=3) ± standard deviation of the mean. Significant differences in comparison to the corresponding control at $p<0.05$:*, $p<0.01$: **, $p<0.001$: *** according to the Student test.

B. Relative *LuPLR1* gene expression determined through RT-qPCR analysis determined 24 h after treatment. **c.** (+)-secoisolariciresinol content quantified by HPLC 96 h after treatment. Data are expressed as the mean of 3 independent experiments ± standard deviation of the mean and different letters indicate significant differences between conditions ($P < 0.05$).

(Color online).

Figure 3. Effect of EGTA and Cd^{2+} on *LuPLR1* gene expression and lignan accumulation in flax cells

A. Effect of EGTA addition (Ca^{2+} chelator) and Cd^{2+} addition (Ca^{2+} competitor) on the ABA-mediated transcription activation of the *LuPLR1* gene. The ß-glucuronidase activity was quantified 48 h after treatment in a stably transformed cell suspension of flax harboring the complete *LuPLR1* gene promoter *GUS* fusion construct. Cells were cultured in incubation medium supplemented with 100 µM ABA and 5 mM Ca^{2+} and subjected to either EGTA addition at 5 mM or Cd^{2+} addition at 2 mM final concentration. CTL corresponds to the control without treatment (DMSO addition).

B. (+)-secoisolariciresinol content quantified by HPLC 96 h after the same treatments described above.

Data are expressed as the mean of 3 independent experiments ± standard deviation of the mean and different letters indicate significant differences between conditions ($P < 0.05$).

(Color online).

Figure 4. Effect of nifedipine (NIF) and heparin (HEP) treatments on cytosolic Ca^{2+} content, *LuPLR1* gene expression and lignan accumulation in flax cells

A. Cell imaging of intracellular fluorescence of the calcium probe Fluo 3-AM in response to an exogenous ABA supply combined with a calcium channel inhibitor. Flax cell suspensions were observed 24 h after probe addition, ABA and inhibitor addition under fluorescent (odd numbers) or visible (even numbers) light. In the negative control, cells were supplemented only with the probe (A1/A2) whereas in the positive control, cells were treated with ABA 100 µM (A3/A4) and the probe. Effect of nifedipine (NIF, a Ca^{2+} influx channel blocker) addition in A5/A6 or heparin (HEP, a Ca^{2+} efflux channel blocker) addition in A7/A8 on ABA-treated flax cells. ABA concentration used was 100 µM.

B. Relative Fluorescence Units of flax cells in response to exogenous ABA supply combined with calcium channel inhibitors (NIF and HEP) determined using a fluorometer after 24 h of treatment corresponding to the relative cytosolic Ca^{2+} concentration.

C. Effect of NIF (25 µM) and HEP (10 µM) addition on the ABA-mediated transcription activation of the *LuPLR1* gene. The ß-glucuronidase activity was determined 48 h after treatment in stably transformed cell suspensions of flax harboring the complete *LuPLR1* gene promoter *GUS* fusion construct. Cells were cultured in incubation medium supplemented with 100 µM ABA and 5 mM Ca^{2+} and subjected to NIF or HEP addition. CTL represents the control without treatment (DMSO addition).

D. (+)-secoisolariciresinol content quantified by HPLC 96 h after the same treatments described above.

Data are expressed as the mean of 3 independent experiments ± standard deviation of the mean and different letters indicate significant differences between conditions ($P < 0.05$).

(Color online).

Figure 5. Effect of staurosporine (STAU) and calmidazolium (CALM) treatments on *LuPLR1* gene expression and lignan accumulation in flax cells

A. Detection of in-gel CDPK activity with varying concentrations of total soluble proteins extracted from ABA-treated cells and impact of STAU, a CDPK inhibitor, addition on this activity (Stau1 and Stau2 corresponding to STAU additions at 5 and 10 µM, respectively.

B. Effect of STAU (5 µM) and CALM, a CaM inhibitor, (25 µM) addition on the ABA-mediated transcription activation of the *LuPLR1* gene. The ß-glucuronidase activity was determined 48 h after treatment in stably transformed cell suspensions of flax harboring the complete *LuPLR1* gene promoter *GUS* fusion construct. Cells were cultured in incubation medium supplemented with 100 µM ABA and 5 mM Ca^{2+} and subjected to either STAU or CALM addition. CTL is the control without treatment (DMSO addition).

C. (+)-secoisolariciresinol content quantified by HPLC 96 h after the same treatments described above.

Data are expressed as the mean of 3 independent experiments ± standard deviation of the mean and different letters indicate significant differences between conditions ($P < 0.05$).

(Color online).

Figure 6. Effects of STAU and CALM treatments combined with ABA supplementation on *LuPLR1* gene expression and lignan accumulation in flax maturing seeds

A. Picture of the experimental procedure for the exogenous application of ABA (100 µM) and 5 mM Ca^{2+} alone or combined with STAU (5 µM) or CALM (25 µM) treatment and seed morphology (SM, developmental stage 2).

B. *LuPLR1* gene expression analyzed by RT-qPCR determined 12 h and 24 h after treatment. CTL is the control without treatment. Data are expressed as the mean of 3 independent experiments ± standard deviation of the mean.

C. (+)-Secoisolariciresinol (in mg/g DW) and ABA (ng/g DW) quantification in treated flaxseed (96h after treatment). CTL is the control without treatment.

Data are expressed as the mean of 3 independent experiments ± standard deviation of the mean. Significant differences in comparison to the corresponding control at p<0.05:*, p<0.01: **, p<0.001: *** according to the Student test.
(Color online).

Figure 7. Roles of ABRE and/or MYB2 *cis*-acting elements in the *LuPLR1* gene promoter activity in flax cell suspensions in response to ABA treatments combined with Ca^{2+} concentration modulators

A. Schematic representations of the different *LuPLR1* gene promoter *GUS* fusion constructs. Crosses indicate mutations in ABRE (A) or MYB2 (M) ABA-response *cis*-acting elements. Lines expressing *GUS* under the wild-type *LuPLR1* promoter (WT), the promoter mutated in ABRE (mABRE), in MYB2 (mMYB2) or in both ABRE and MYB2 (mABRE/MYB2) were used.

B. ß-glucuronidase activity in transformed cell suspensions, expressing the different *pLuPLR1:GUS* constructs treated with ABA 100 µM, 5 mM Ca^{2+} and subjected to Ca^{2+} concentration modulators (EGTA, nifedipine (NIF), heparin (HEP), calmidazolium (CALM) and staurosporine (STAU)). CTL is the control without treatment (DMSO addition).
Data are expressed as the mean of 3 independent experiments ± standard deviation of the mean. Significant differences in comparison to the corresponding control at: p<0.05:*, p<0.01: **, p<0.001: *** according to the Student test.
(Color online).

Figure 8. Implication of CML15b in the Ca2+ signaling regulating the ABA-activation of lignan biosynthesis in flax.

A. Co-expression network of flax lignan biosynthetic genes *LuDIR5*, *LuPLR1* and *LuUGT74S1* with putative Ca^{2+} sensor genes during flax seed development extracted from public RNAseq data and constructed using Cytoscape software. Only positive correlations with a cut-off value of 0.95 for the Pearson correlation coefficients were visualized. Colors from yellow to red indicate increasing Pearson correlation values and the connection size indicates the strength of the connection.

B. Relative gene expression of *LuDIR5*, *LuPLR1*, *LuUGT74S1* and *CML15b* during flax seed development.

C. Schematic diagram of the T-DNA region from binary vector for RNAi CML15b.The hairpin construct consisted of a 155bp sequence of the CML15b gene in sense and antisense orientation and separated by an intron. P35S, promoter of the Cauliflower Mosaic Virus 35S RNA gene; OCS-ter, 3'end of the octopine synthase gene; E-GFP: enhanced green fluorescence protein; P-nos and 3'nos, nopaline synthase gene promoter and 3'end respectively; nptII: coding sequence of the neomycin phosphotransferase gene; LB, RB: T-DNA left and right borders.

D. Transiently transformed cells expressing CML15b-RNAi construction. Cells were observed under bright field or fluorescence microscopy (using a 488 nm excitation filter and a 540 nm wavelength pass filter).

E. Relative *CML15b* gene expression analyzed by RT-qPCR determined 24 h after treatment with mock (DMSO) or 100µM ABA and 5 mM Ca^{2+} in wild type (WT) and RNAi-CML15b transgenic flax cells.

F. Relative *LuPLR1* gene expression analyzed by RT-qPCR determined 24 h after treatment with mock (DMSO) or 100µM ABA and 5 mM Ca^{2+} in wild type (WT) and RNAi-CML15b transgenic flax cells.

G. (+)-Secoisolariciresinol (in mg/g DW) HPLC quantification in wild type (WT) and RNAi-CML15b transgenic flax cells 96h after treatment.

Data are expressed as the mean of 3 independent experiments ± standard deviation of the mean and different letters indicate significant differences between conditions ($P < 0.05$).

(Color online).

Figure 9. Proposed gene regulatory mechanism model for the role of Ca^{2+} in the ABA-mediated *LuPLR1* gene expression. ABA: Abscisic Acid; ABFs: ABRE Binding Factors; ABRE: ABA-Response Element; CaM: Calmodulin; CML15b: Calmodulin 15b; Cd^{2+}: Cadmium; CDPKs: Ca^{2+}-dependent protein kinases; InsP3: Inositol Triphosphate; *LuPLR1*: *Pinoresinol Lariciresinol Reductase 1* encoding gene from *Linum usitatissimum*; MYB2: MYB2 TF-binding site; TF: Transcription Factor.

(Color online).

Figure 1

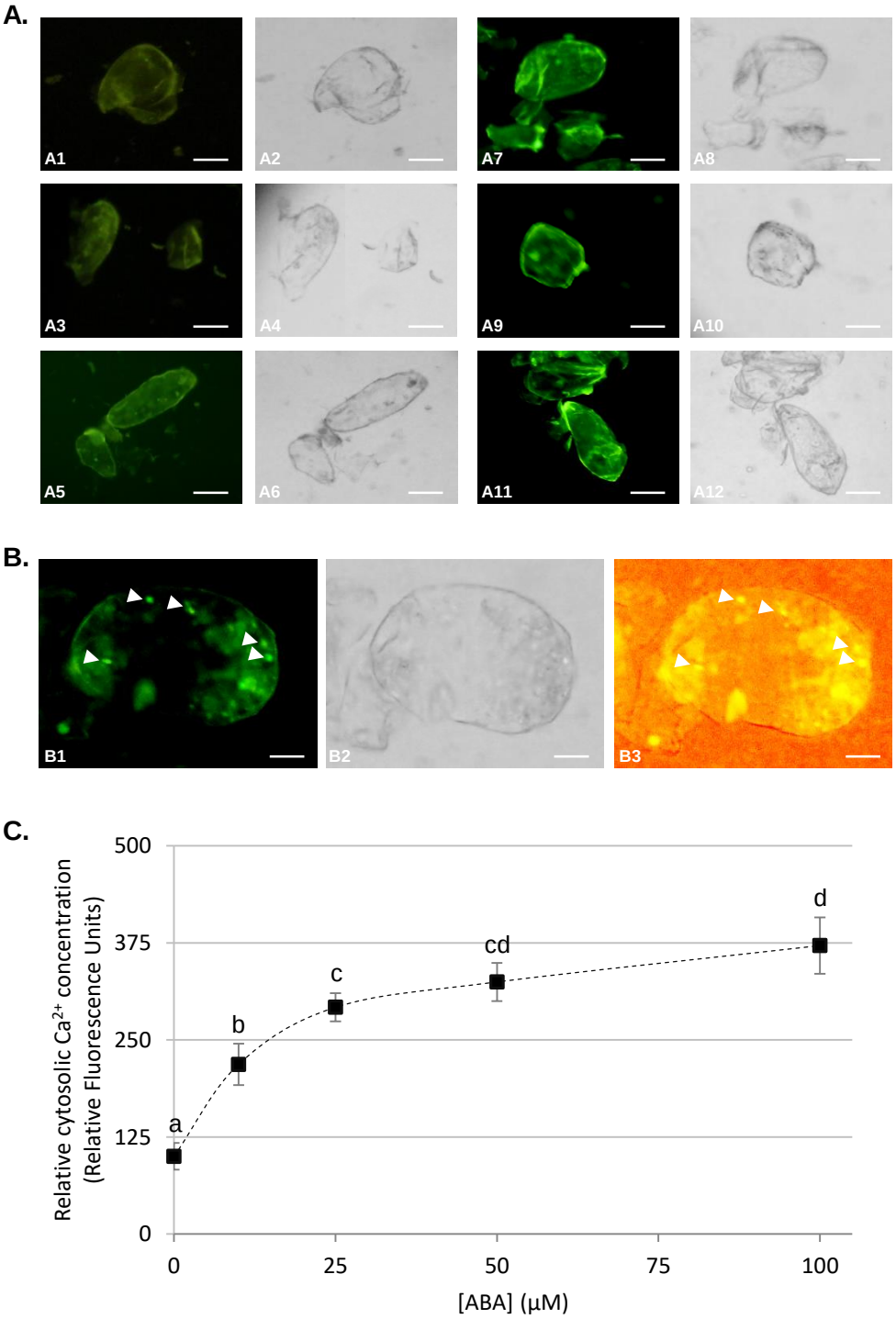
A.
A1
A2
A7
A8
A3
A4
A9
A10
A5
A6
A11
A12
B.
B1
B2
B3
C.
Relative cytosolic Ca2+ concentration
(Relative Fluorescence Units)
500
375
250
125
0
a
b
c
cd
d
0
25
50
75
100
[ABA] (µM)

Figure 2

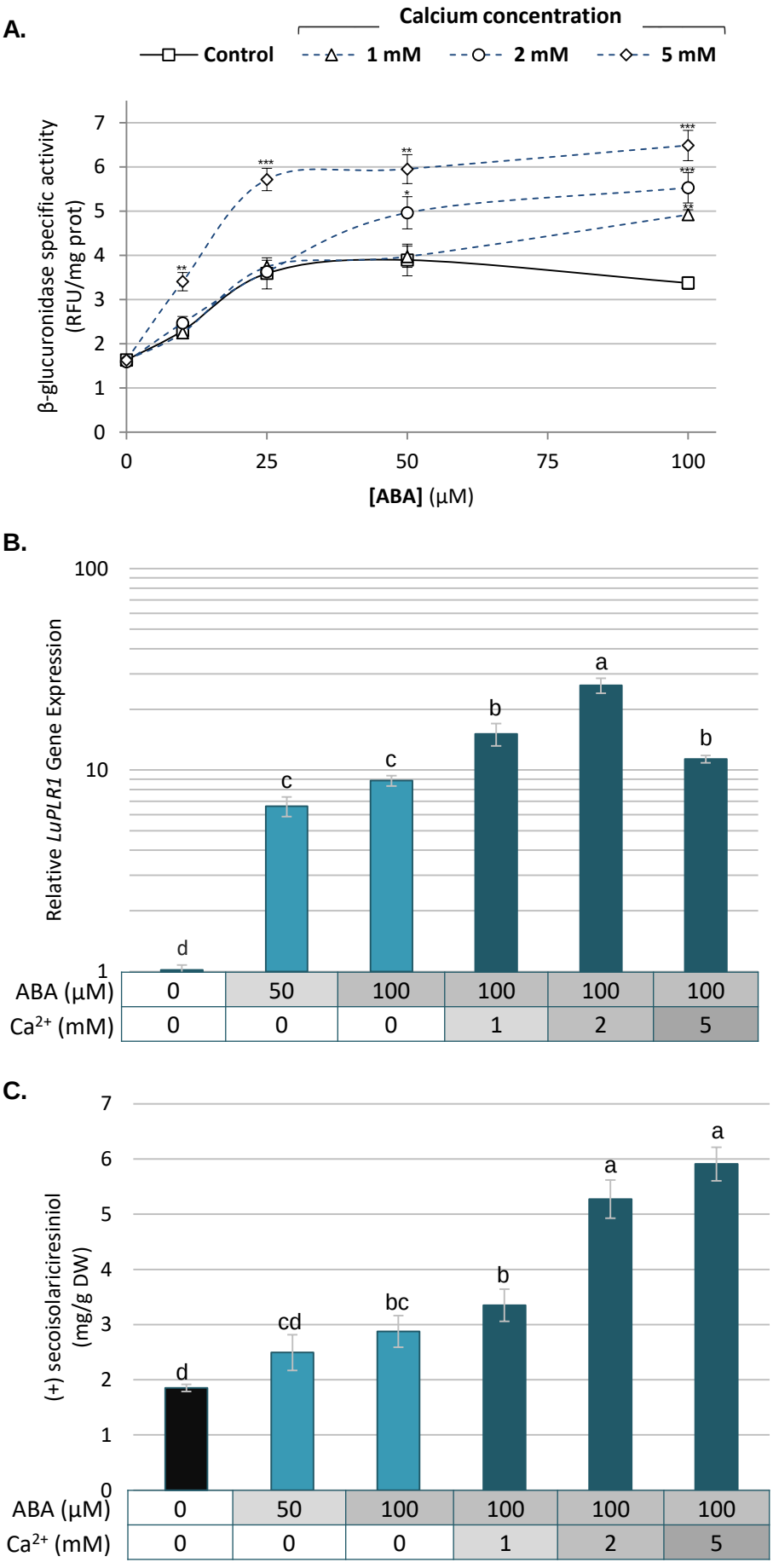
A.
Calcium concentration
Control
1 mM
2 mM
5 mM
β-glucuronidase specific activity (RFU/mg prot)
[ABA] (µM)
B.
Relative LuPLR1 Gene Expression
ABA (µM)
Ca2+ (mM)
C.
(+) secoisolariciresiniol (mg/g DW)
ABA (µM)
Ca2+ (mM)

Figure 3

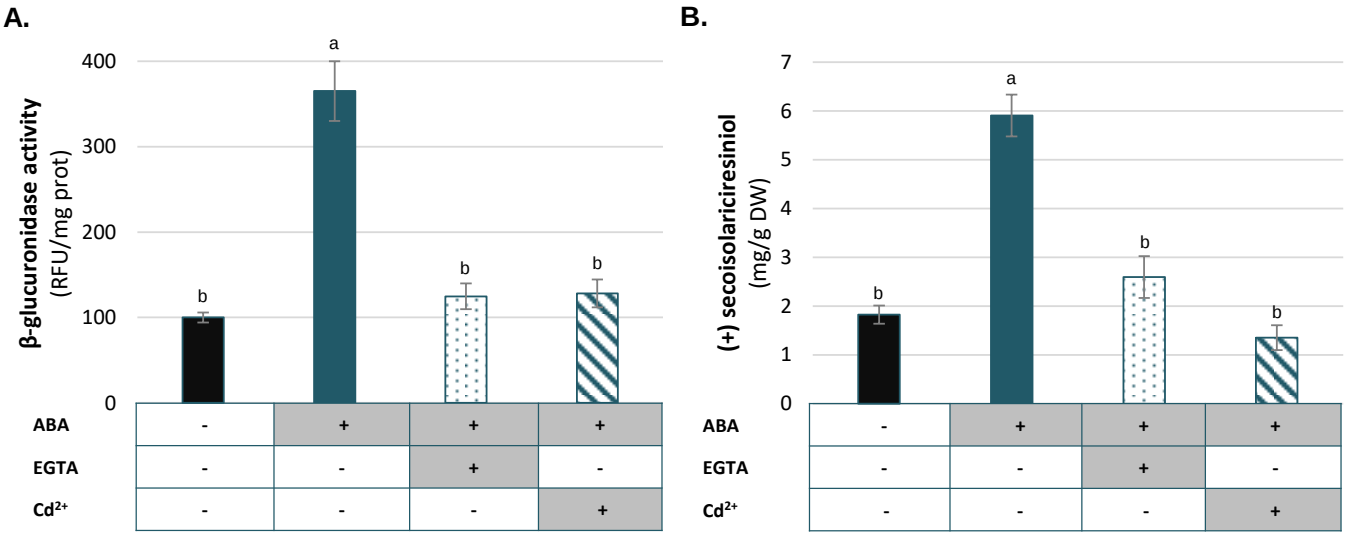
A.
β-glucuronidase activity
(RFU/mg prot)
400
300
200
100
0
a
b
b
b
ABA
EGTA
Cd2+
B.
(+) secoisolariciresiniol
(mg/g DW)
7
6
5
4
3
2
1
0
a
b
b
b
ABA
EGTA
Cd2+

Figure 4

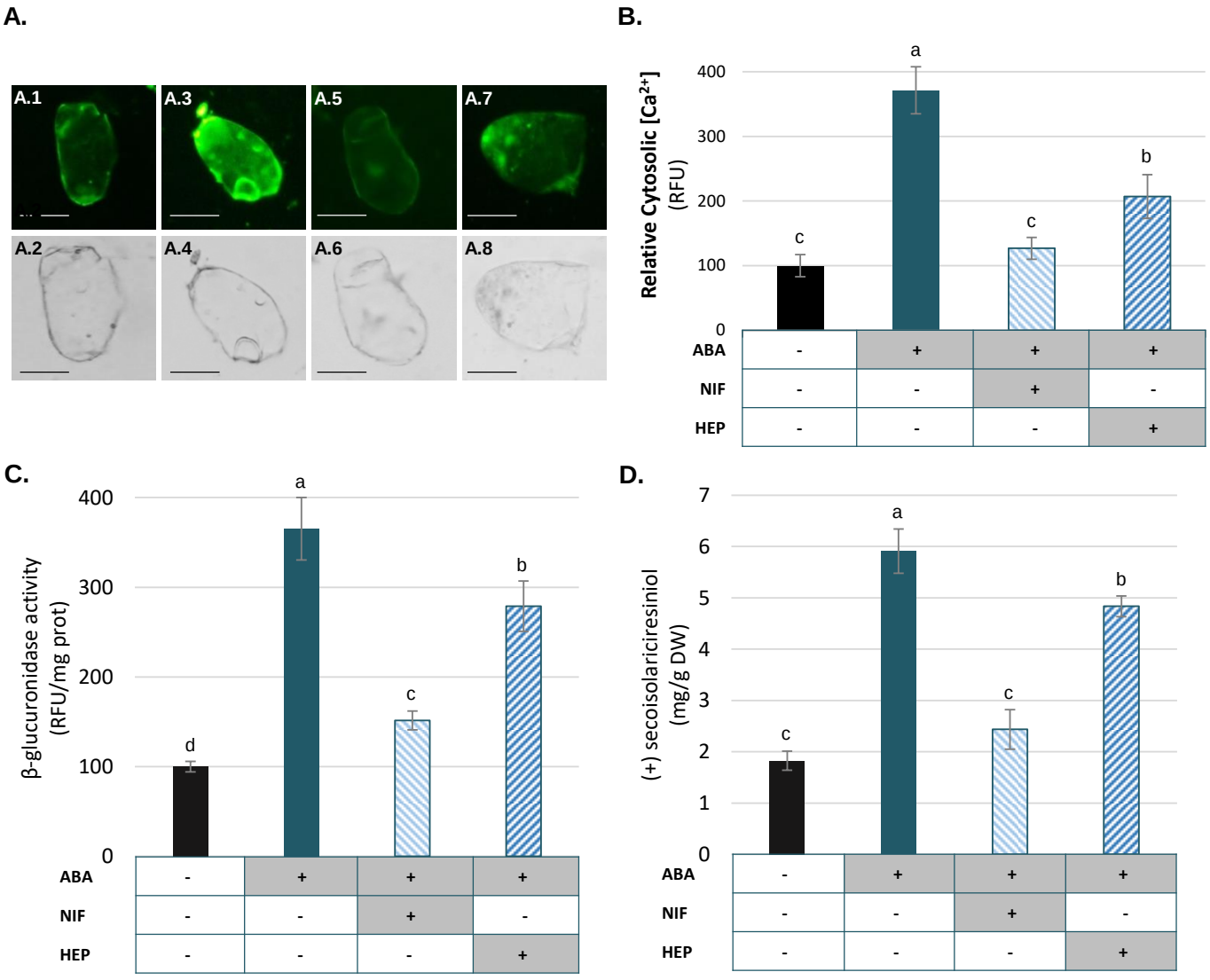
A.
A.1
A.3
A.5
A.7
A.2
A.4
A.6
A.8
B.
Relative Cytosolic [Ca2+] (RFU)
400
300
200
100
0
a
b
c
c
ABA - + + +
NIF - - + -
HEP - - - +
C.
β-glucuronidase activity (RFU/mg prot)
400
300
200
100
0
a
b
c
d
ABA - + + +
NIF - - + -
HEP - - - +
D.
(+) secoisolariciresiniol (mg/g DW)
7
6
5
4
3
2
1
0
a
b
c
c
ABA - + + +
NIF - - + -
HEP - - - +

Figure 5

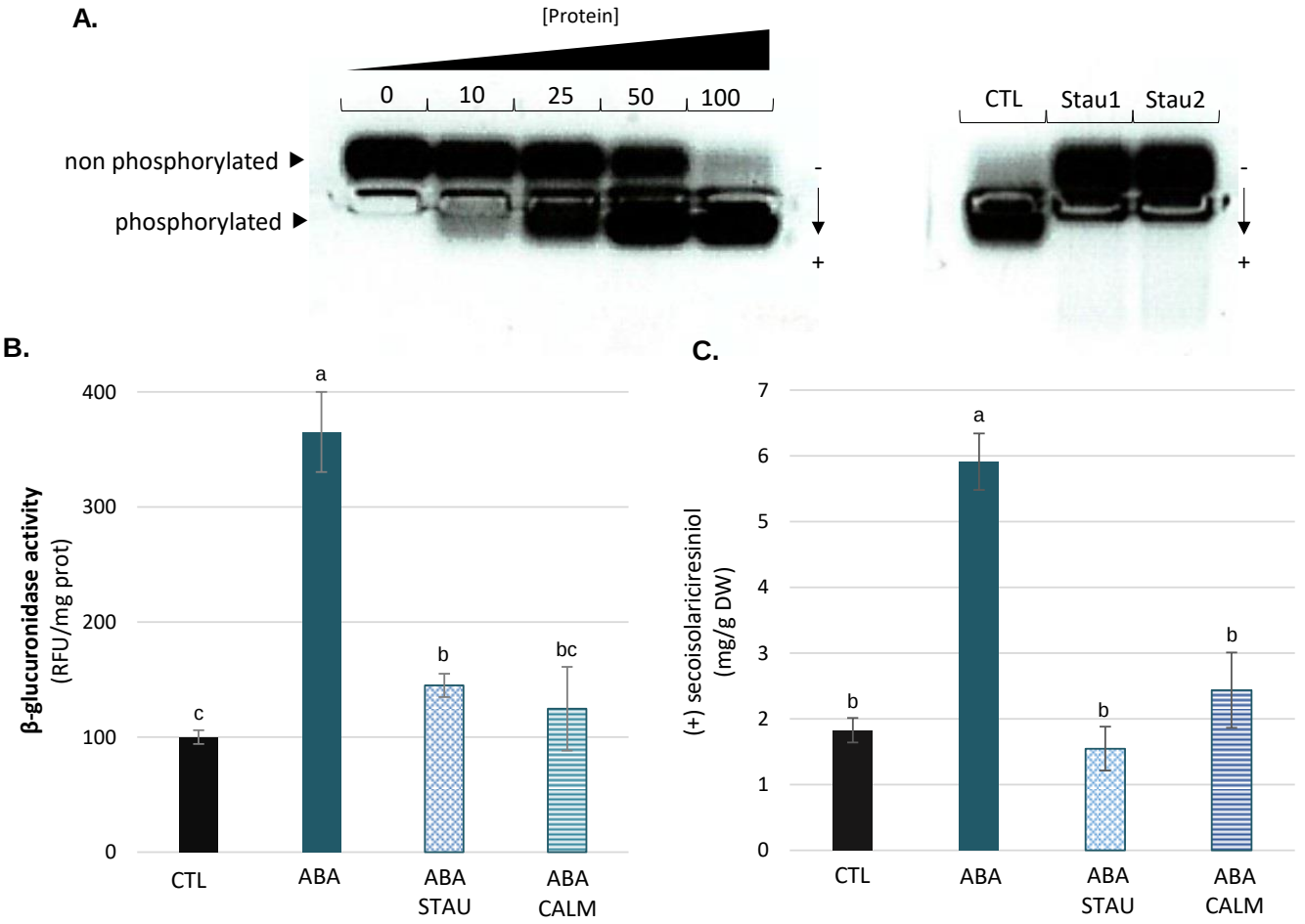
A.
[Protein]
0
10
25
50
100
non phosphorylated
phosphorylated
-
+
CTL
Stau1
Stau2
-
+
B.
β-glucuronidase activity
(RFU/mg prot)
400
300
200
100
0
a
b
bc
c
CTL
ABA
ABA STAU
ABA CALM
C.
(+) secoisolariciresiniol
(mg/g DW)
7
6
5
4
3
2
1
0
a
b
b
b
CTL
ABA
ABA STAU
ABA CALM

Figure 6

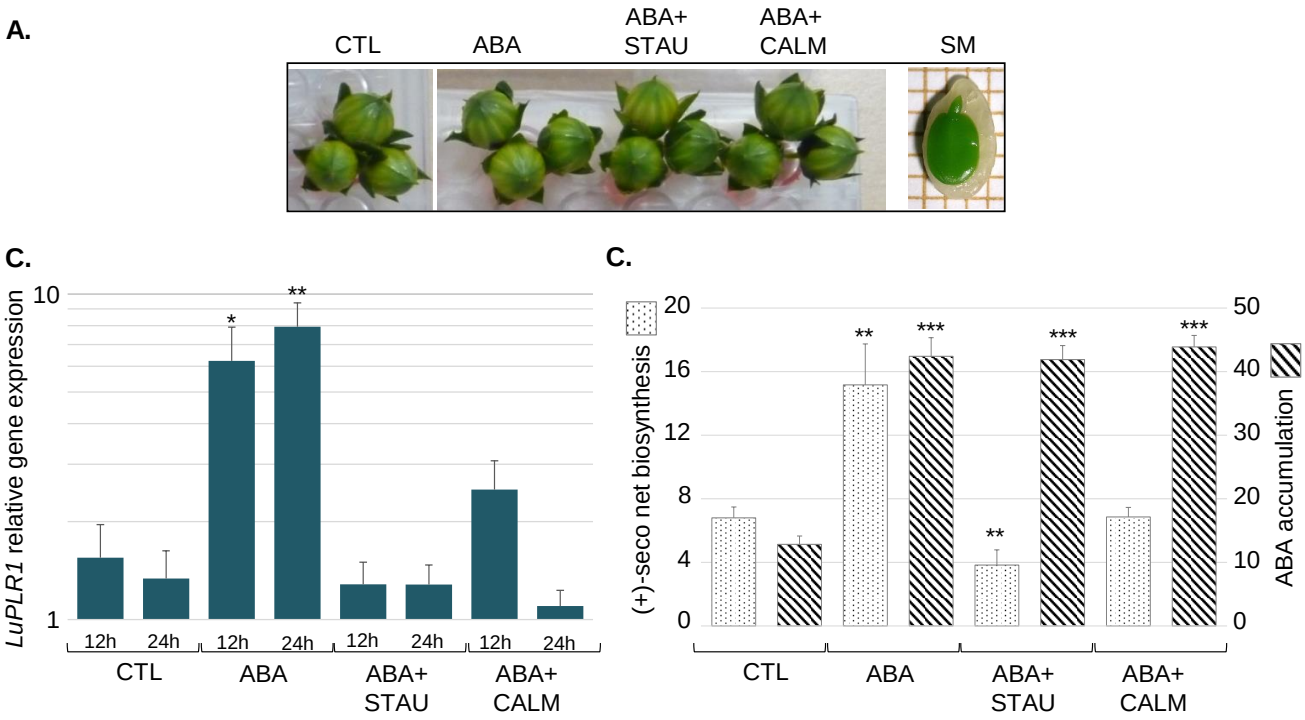
A.
CTL
ABA
ABA+ STAU
ABA+ CALM
SM
C.
LuPLR1 relative gene expression
10
1
*
**
12h
24h
CTL
ABA
ABA+ STAU
ABA+ CALM
C.
(+)-seco net biosynthesis
ABA accumulation
20
16
12
8
4
0
50
40
30
20
10
0
**
***
**
***
***
CTL
ABA
ABA+ STAU
ABA+ CALM

Figure 7

A.

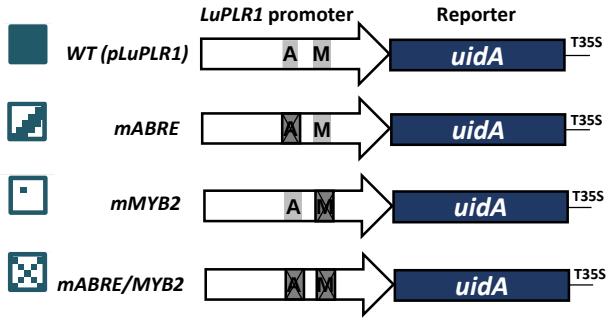

B.

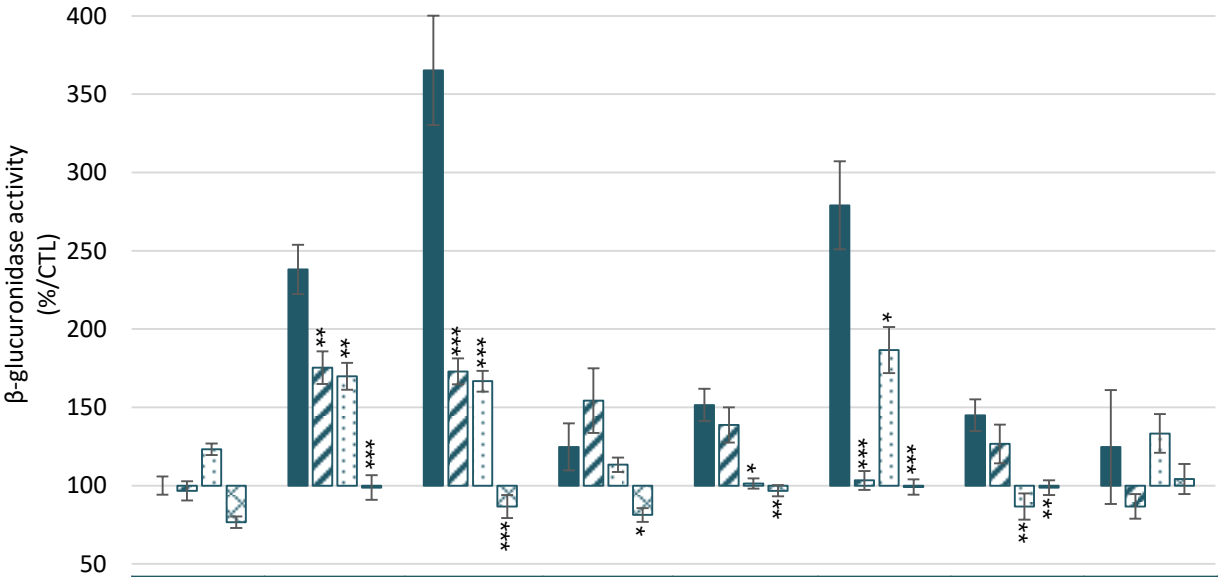

ABA	-	+	+	+	+	+	+	+
Ca^{2+}	-	-	+	+	+	-	+	+
EGTA	-	-	-	+	-	-	-	-
NIF	-	-	-	-	+	-	-	-
HEP	-	-	-	-	-	+	-	-
STAU	-	-	-	-	-	-	+	-
CALM	-	-	-	-	-	-	-	+

Figure 8

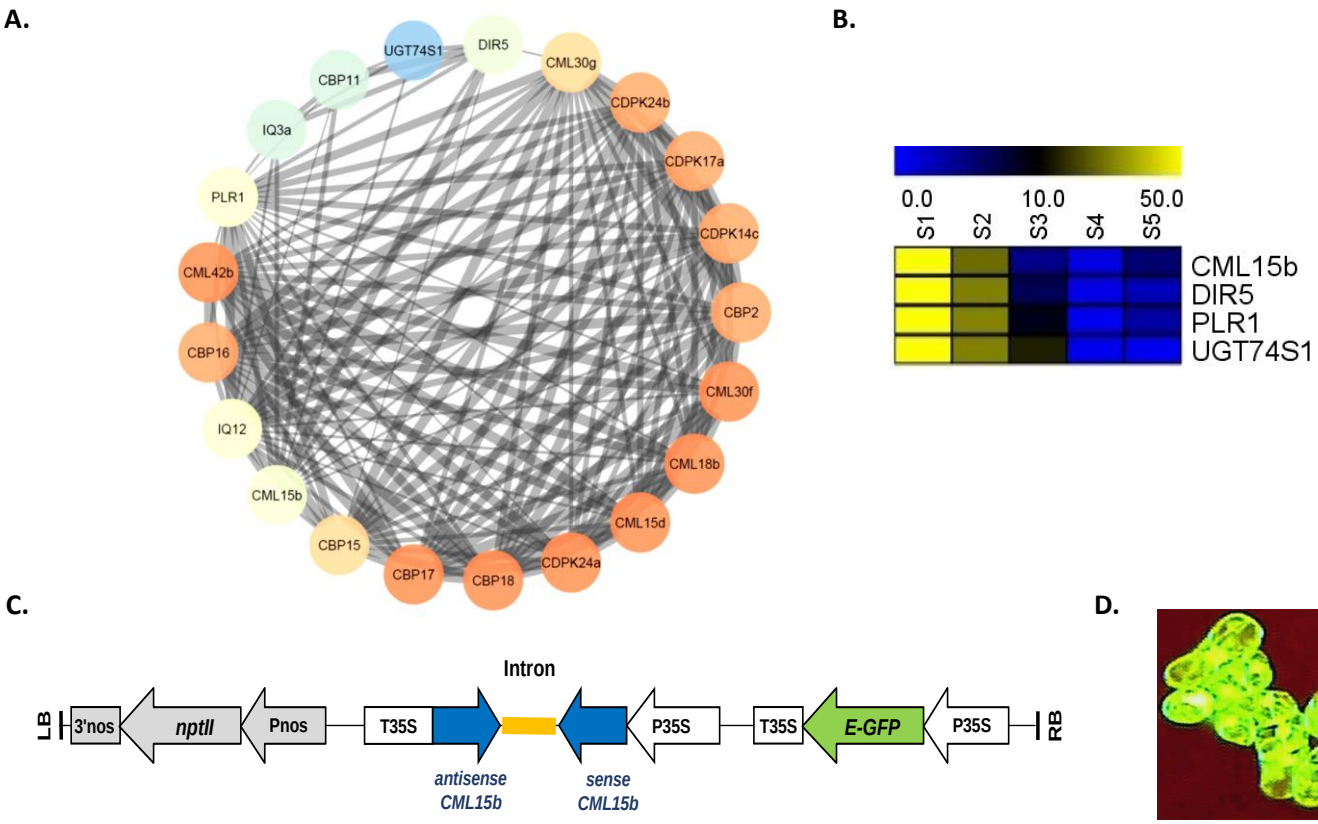
A.
UGT74S1
DIR5
CML30g
CBP11
CDPK24b
IQ3a
CDPK17a
PLR1
CDPK14c
CML42b
CBP2
CBP16
CML30f
IQ12
CML18b
CML15b
CML15d
CBP15
CBP17
CBP18
CDPK24a
B.
0.0
10.0
50.0
S1
S2
S3
S4
S5
CML15b
DIR5
PLR1
UGT74S1
C.
Intron
LB
3'nos
nptII
Pnos
T35S
P35S
T35S
E-GFP
P35S
RB
antisense CML15b
sense CML15b
D.

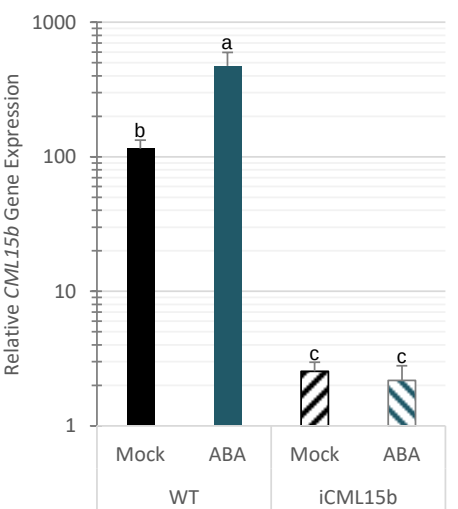
E.
Relative CML15b Gene Expression
1000
100
10
1
a
b
c
c
Mock
ABA
Mock
ABA
WT
iCML15b

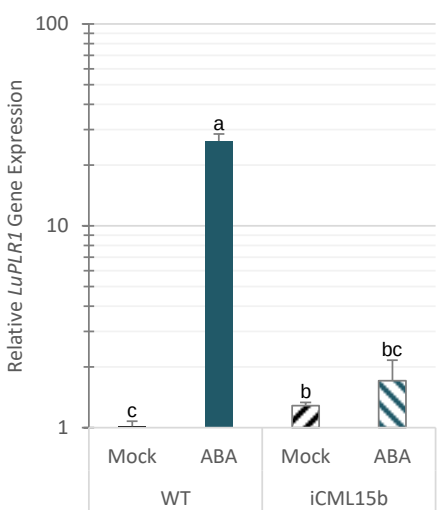
F.
Relative LuPLR1 Gene Expression
100
10
1
a
c
b
bc
Mock
ABA
Mock
ABA
WT
iCML15b

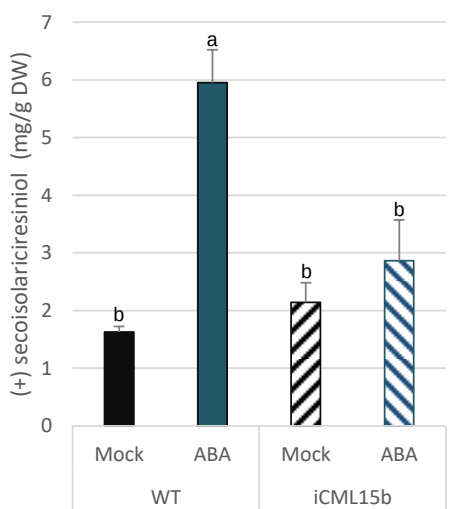
G.
(+) secoisolariciresiniol (mg/g DW)
7
6
5
4
3
2
1
0
a
b
b
b
Mock
ABA
Mock
ABA
WT
iCML15b

Figure 9

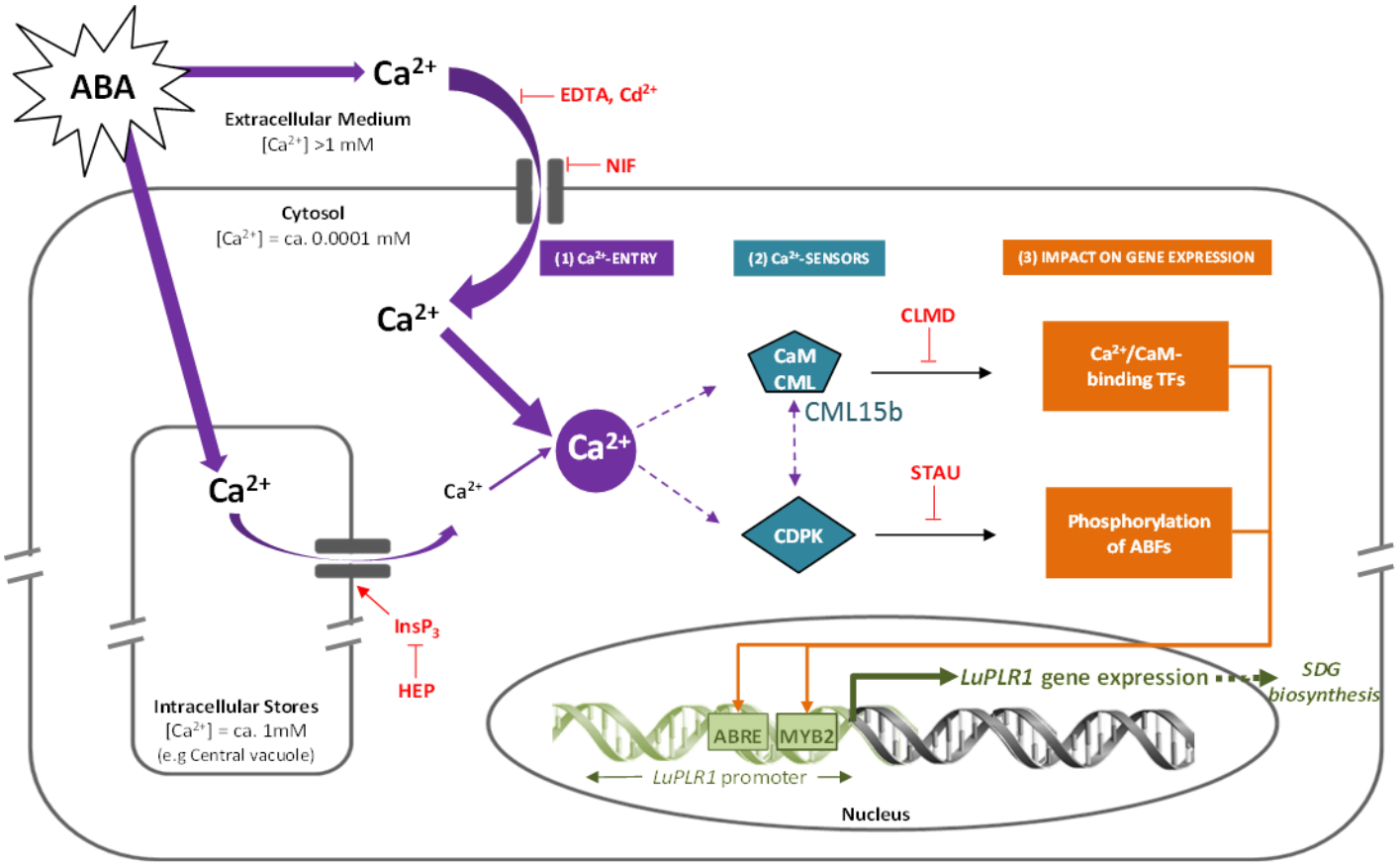
ABA
Ca2+
Extracellular Medium
[Ca2+] >1 mM
EDTA, Cd2+
NIF
Cytosol
[Ca2+] = ca. 0.0001 mM
(1) Ca2+-ENTRY
(2) Ca2+-SENSORS
(3) IMPACT ON GENE EXPRESSION
Ca2+
CaM
CML
CLMD
Ca2+/CaM-binding TFs
CML15b
Ca2+
Ca2+
Ca2+
STAU
CDPK
Phosphorylation of ABFs
InsP3
HEP
Intracellular Stores
[Ca2+] = ca. 1mM
(e.g Central vacuole)
LuPLR1 gene expression
SDG biosynthesis
ABRE
MYB2
LuPLR1 promoter
Nucleus